Chapter 14
Models of Liquid Crystalline Polymer Fibers

J.I. Ramos

14.1 Introduction

Many materials used in industry, e.g., high-performance tires and cables, light-weight and super-strength materials, etc., used, for example, in bullet-proof vests, stealth technology, etc., are manufactured from liquid crystalline polymer fibers. These fibers are in turn manufactured by means of fiber-spinning processes whereby a high-temperature liquid phase of rigid rod macromolecules is extruded trough a die, cools as it is being pulled downstream, solidifies, and is collected in a rotating drum.

The properties of the collected fiber depend on the morphology of the amorphous and semi-crystalline phases; the morphology, in turn, depends on the thermal and deformation histories undergone by the material during processing. In many cases, fibers and films are subjected to large inelastic deformations after manufacture, and, during the course of these deformations, further crystallization may take place.

The remarkable strength properties of LCP spun fibers are mainly due to the molecular alignment of the macromolecules which is achieved as a result of the complex interactions among the flow, stresses, molecular orientation, crystallization, and thermal processes at play in fiber-spinning processes and, in particular, the coupling between the molecular orientation and the elongational characteristics of the flow. For example, ultra-strength textile fibers such as Vectran and Kevlar (Chawla 1998) achieve their properties, e.g., tensile modulus, as a result of the interaction between the anisotropic molecular-scale structure of the melt or solution, the macroscopic hydrodynamics of spinning flows and non-isothermal effects

J.I. Ramos (✉)
Escuela de Ingenierías, Universidad de Málaga, Room 2-139-D, Dr. Ortiz Ramos, s/n, Málaga 29071, Spain
e-mail: jirs@lcc.uma

V.K. Thakur, M.R. Kessler (eds.), *Liquid Crystalline Polymers*,
DOI 10.1007/978-3-319-22894-5_14

including radial heat transfer through the fiber free surface, temperature dependence of material properties, phase change, and crystallization.

The properties of LCP fibers depend strongly on their molecular orientation; a high degree of orientation results in high strength and stiffness along the alignment direction, i.e., along the fiber in melt spinning, but it also yields anisotropic properties (Ramalingam and Armstrong 1993) that may be detrimental when multidimensional stability, e.g., absence of shrinkage and warping, and strength are required.

Liquid-crystalline solutions may phase separate even under isothermal conditions due to electrostatic and steric interactions that result from the rigidity of the polymer chain backbones even at low polymer concentrations, and form anisotropic phases with a degree of molecular orientation even in the quiescent state as evidenced by their ability to exhibit birefringence under static conditions.

For isothermal flows at low shear rates, a nematic LCP may be called flow-aligning because shear promotes the alignment of the nematic director at an angle with respect to the flow direction, but shear may also result in tumbling which is characterized by a continuous rotation of the director (Greco and Marrucci 1993).

Although considerable progress has been made in the understanding and modeling the molecular orientation of lyotropic solutions of rod-like polymers, the situation is not yet as advanced in the case of thermotropic LCP.

The rate of crystallization of semi-crystalline polymers depends on the molecular orientation in the melt; when subject to deformations that align the polymer molecules, the rate of crystallization increases dramatically, and, when the temperature drops below the glass transition temperature, there is a cessation of molecular motion and the crystallization rate decreases and may stop. As the crystallinity increases, it retards the crystallization process and decreases the mobility of the polymer molecules in the amorphous phase. The molecular orientation and crystallization affect and are affected by the melt rheology and thermal field.

Experimental studies indicate that flow-induced crystallization correlates with the viscoelastic stresses much more strongly than with the macroscopic strain or strain rate, thus indicating that the molecular chain orientation and extension are of paramount importance in determining the fiber's final morphology.

The relations among the flow, strain rate, cooling, molecular orientation, crystallization and rheology of LCP is a complex one, depends on many factors, and is not yet clear due to the complex interactions amongst these phenomena, although great strides have been made in understanding the relation between molecular weight distribution and linear viscoelastic properties of polymers (Pattamaprom et al. 2000, 2008), and that between rheology and flow-induced nucleation (Eder and Janeschitz-Kriegl 1997).

In this chapter, a review of models of fiber spinning of liquid crystalline and semi-crystalline polymers is presented. Since, as stated above, the flow, crystallization, molecular orientation, rheology and the thermal field play a paramount role in determining the properties and morphology of both LCP and liquid semi-crystalline fibers, it was believed to be convenient to first review and extend some of the crystallization models that have been developed for both quiescent

and flow conditions; this is done in Sect. 14.2. Some models for the molecular orientation are described in some detail in Sect. 14.3, while the effects of both the molecular orientation and the crystallization on the rheology of both LCP and liquid semi-crystalline polymers are summarized in Sect. 14.4. Even though, some models for the fiber spinning of LCP are described in Sects. 14.2–14.4 with reference to the models for the crystallization, molecular orientation and rheology, the main one- and two-dimensional models that have been developed to-date for fiber spinning of thermotropic LCP and liquid semi-crystalline polymers are reviewed in Sect. 14.5. Some conclusions and areas for future work are summarized in Sect. 14.6.

14.2 Crystallization Models

Polymers that are unable to crystallize on cooling below their glass transition temperature form amorphous solids and may exhibit strong anisotropy if these solids are formed by deforming the polymer while cooling it through the glass transition temperature. As the deformed amorphous polymer melt cools below its glass transition temperature, its molecules lose their mobility and become frozen in their oriented configuration.

Some polymers, e.g., polyethylene (PE), find applications at temperatures between their melting and glass transition temperatures. At these temperatures, the solid consists essentially of rigid crystals and a flexible amorphous phase, and it is therefore solid and tough.

Polymers having a regular or ordered molecular structure may form a semi-crystalline solid when kept at a temperature below the melting one for a sufficiently long time. The crystallization process can be very slow especially at temperatures just below the equilibrium melting temperature, and the resulting solid has a spherulitic morphology under quiescent conditions.

In the liquid phase, there are always density fluctuations caused by thermal agitation (Landau and Lifshitz 1980a, b). These fluctuations may eventually create small clusters or aggregates of polymer molecules having the same properties as the crystalline phase; small crystals are continuously being created and destroyed by fluctuations because the formation of a crystal involves the creation of an interface between the liquid and the crystal and its consequent energy cost, i.e., the creation of crystals is a competitive process whereby there is a decrease of energy due to the fact that the chemical potential of the crystal phase is lower than that of the liquid, and an increase of energy and an energy cost associated with the creation of interfaces.

Surface effects are dominant in clusters of small size and, therefore, their growth is not energetically favorable, and small crystals tend to dissolve. There exists, however, a critical size beyond which volume effects dominate over surface ones, and the growth of the cluster is favored by a global reduction of energy. The size that determines the stability of the clusters is called critical size, and the process of

formation of crystals of size larger than or equal to the critical size is called nucleation.

Nucleation is the first step in the crystallization process, determines the appearance of the first crystal nuclei which are the germ of the second stage of crystallization, i.e., growth, and is an activated process where an energy barrier has to be overcome in order to form nuclei of a critical size, beyond which the new phase grows spontaneously.

There are two basic types of nucleation: primary nucleation which occurs when nuclei form in the absence of already formed crystals, and secondary nucleation which refers to the formation of nuclei in the presence of already formed crystals. Primary nucleation can occur through two different mechanisms: homogeneous and heterogeneous nucleation. Homogeneous nucleation occurs in the bulk of a pure substance and is the process whereby nuclei are formed spontaneously from a supersaturated solution that has crossed the metastable limit, whereas heterogeneous nucleation takes place in the presence of impurities, pre-existing crystals, boundaries, etc. Secondary crystallization can occur through surface, contact, fracture, pressure, strain, attrition, etc., mechanisms (Schultz 2001).

In the growth stage, nuclei larger than the critical size tend to grow either through the addition of monomers or by acting as sites of heterogeneous nucleation, e.g., nucleation on the surface of a growing crystal. Crystals grow freely until they begin to completely fill the whole space. Once they hit each other, their growth stops at the contact surface. This phenomenon, referred to as impingement, determines the final morphology of the processed polymer.

In the final stage of crystallization, crystal impingement impedes the subsequent nucleation of the crystals and, therefore, amorphous matter remains trapped among clusters. Furthermore, the clusters themselves are not fully crystalline because they may contain some amorphous inclusions. This trapped material can eventually join the main crystal structure and, therefore, increase the degree of crystallization in a process referred to as secondary crystallization (Schultz 2001).

Models for the crystallization of polymers have been mainly based on the Avrami-Kolmogorov equation (Kolmogorov 1937; Avrami 1939, 1940, 1941; Johnson and Mehl 1939; Evans 1945) that is based on the theory of filling the space through the nucleation and growth of one phase into another. This equation was initially developed for isothermal, quiescent crystallization, although, as described below, it has been extended to account for non-isothermal conditions.

In quiescent crystallization, polymer crystallization from the melt is usually dominated by heterogeneous nucleation. Nuclei grow in time depending on the pressure and temperature, and form spherulites that impinge upon each other and stop growing when complete space filling is reached; crystalline lamellae grow in three dimensions starting from point-like nuclei (Burger et al. 2002; Capasso 2003; Eder 1997).

Although many attempts have been made to model the crystallization process in semi-crystalline polymers under quiescent conditions, most models do not account for the polymorphism in a clear way or do not account for the relevant processing conditions, e.g., pressure. Drawing experiments on poly(ethylene 2,6-naphthalene

dicarboxylate) (PEN) fibers indicate that the crystal structure depends on the drawing stress, i.e., depending on the magnitude of the stress, α- and/or β-crystals may form (Kim et al. 2012). In addition the drawing stress was observed to have a great influence not only on the resulting crystal form but also on the chain conformation of the mesophase structure.

In polymorphic materials, the crystallization kinetics of different polymorphs is not well-established as a function of the pressure and temperature. In some cases, an increase of the pressure results in an increase of both the nucleation density and the equilibrium melting temperature and, therefore, a higher undercooling that it is the driving force for crystallization; however, the exact effect of the pressure on the growth rate of a given crystal is not yet known.

For nylon 6, Shanon et al. (2000) found that the onset time for crystallization in melt spinning depends chiefly on chain orientation and not appreciably on chain chemistry or specific undercooling; this result is consistent with a critical strain condition.

When phase transitions occur in a flowing polymer melt, crystallization takes place under strain and non-isothermal conditions, and the morphology of the processed polymer depends on the temperature and deformation history. In fact, it has been observed experimentally that crystallization is influenced strongly by the flow, stress, temperature and molecular orientation (Ziabicki 1974, 1976) and may be enhanced by shear, pressure and strain, and shear may increase the nucleation density, whereas the crystallization rate decreases as the cooling rate is increased. Furthermore, a highly oriented crystalline morphology is usually obtained under isothermal and non-isothermal deformations, in contrast with the spherulite morphology observed under quiescent conditions, and both the alignment and the orientation increase as the shear rate is increased (Vaish et al. 2001). In spun fibers, for example, lamellae are found to be perpendicular to the fiber axis and enhanced crystallization is caused by chain extension arising from entanglement between molecules.

Molecular orientation in the melt usually accelerates the phase transition process, but the molecular orientation may be enhanced or relaxed depending on the deformation history and the relaxation times of the melt. This means that models of fiber spinning processes should account for the molecular orientation and its effects on the flow field, stress and crystallization, and also for the effects of these fields on the molecular orientation.

A model of polymer crystallization under both quiescent and flow conditions should also account for the nucleation density and the spherulitic growth rates and include secondary crystallization.

As stated above, many of the crystallization models employed to study fiber spinning processes of semi-crystalline polymers are based on non-isothermal generalizations of the Avrami-Kolmogorov's kinetics model for quiescent crystallization where space filling is given by

$$\alpha(t) = \frac{\theta(t)}{\theta_\infty} = 1 - \exp(-\phi_0\,(t)), \tag{14.1}$$

t is time, $\theta(t)$ and θ_∞ are the crystallized volume fractions at time t and under equilibrium conditions, respectively, and $\phi_0(t)$ is the sum of the expected crystallized volumes of the different phases if no impingement occurs in the case of three-dimensional spherulitic growth, i.e.,

$$\phi_0\,(t) = \sum \phi_{0i}(t). \tag{14.2}$$

14.2.1 Avrami-Kolmogorov Kinetics for Quiescent Crystallization and Generalizations

In the original Kolmogorov's formulation (Kolmogorov 1937) only quiescent crystallization was considered and the crystallinity fraction is

$$\alpha = 1 - \exp\left(-\alpha_{af}\right), \tag{14.3}$$

where

$$\alpha_{af} = C_m \int_0^t \frac{dN}{ds}(s)ds \left[\int_s^t G(u)du\right]^m, \tag{14.4}$$

m denotes the (constant) dimensionality of the crystallites, $\frac{dN}{dt}$ is the rate of nuclei production and $G(t)$ is the linear growth rate; $m = 3$ for spherical crystals and $C_m = 4\pi/3$, although m may range from 1 to 3 and is not necessarily an integer number.

In the Kolmogorov model, nucleation is assumed to occur randomly and homogeneously over the entire untransformed portion of the material, the growth rate does not depend on the extent of transformation, growth occurs at the same rate in all directions, and only the transformation of a phase into another one is considered.

For constant growth rates, the second integral of (14.4) can be performed exactly. Moreover, if an isokinetic approach is considered whereby the growth rate is proportional to the nucleation one and the latter is constant, one may easily derive the well-known Avrami's expression (Avrami 1939, 1940, 1941; Johnson and Mehl 1939; Evans 1945).

The Avrami-Kolmogorov kinetic model can be extended to account for both thermal and flow-induced crystallization by simply considering that the number of nuclei is $N = N_0 + N_f$, where N_0 denotes the number of nuclei created under quiescent conditions and N_f is the number of the flow-created nuclei. N_0 depends on the temperature, i.e., thermal nucleation, while the growth rate for flow-induced crystallization may be assumed to vary linearly with the shear rate.

If the growth rate for the flow-induced crystallization is assumed to be only a function of the temperature and we assume that (Eder and Janeschitz-Kriegl 1997)

$$\frac{dN_f}{dt} + \frac{N_f}{\tau} = g, \tag{14.5}$$

where τ is a temperature-dependent relaxation time and g usually depends on the flow variables and the temperature, τ and g are assumed to be constant and $N_f\,(0) = 0$, then (14.5) yields

$$N_f\,(t) = \tau\, g\left(1 - \exp\left(-\frac{t}{\tau}\right)\right). \tag{14.6}$$

For isothermal flows and $G(t)$ constant, one can easily obtain from (14.3) and (14.4)

$$\alpha = 1 - \exp\left(-C_m\, G^m \int_0^t \frac{dN}{ds}(s)(t-s)^m\, ds\right), \tag{14.7}$$

that, on accounting for the quiescent crystallization at a constant nucleation rate, yields

$$\alpha = 1 - \exp\left(-C_m\, G^m \left[K\, t^{m+1} + \int_0^t \frac{dN_f}{ds}(s)(t-s)^m\, ds\right]\right). \tag{14.8}$$

Equation (14.8) reduces to the well-known Avrami-Kolmogorov's kinetics in the absence of flow-induced crystallization, i.e., for $\frac{dN_f}{dt}\,(t) = 0$ (Avrami 1939, 1940, 1941; Johnson and Mehl 1939).

Equation (14.8) may be written as $\alpha = 1 - \exp(-\phi_0\,(t))\exp(-\varphi_0\,(t))$, where the first and second exponential terms are associated with the thermal and flow-induced crystallizations, respectively; the former is usually modelled by means of the Avrami-Kolmogorov kinetics, whereas several models have been proposed for the latter, as discussed below.

If the exponential terms are sufficiently small, (14.8) can be written as $\alpha \approx (1 - \exp(-\phi_0\,(t)))(1 - \exp(-\varphi_0\,(t))) = \alpha_t(t)\alpha_f(t)$, where α_t and α_f refer to the crystallization fractions associated with temperature and flow, respectively.

Under isothermal conditions with constant $G(t)$, the Avrami-Kolmogorov's generalized expression, i.e., (14.4) and (14.8), for flow-induced crystallization may be written as

$$\alpha_f = C_m\, G^m \int_0^t \frac{dN_f}{ds}(s)(t-s)^m\, ds, \tag{14.9}$$

which upon repeated differentiation with respect to time yields

$$\frac{d\alpha_f}{dt} = m\, C_m\, G^m \int_0^t \frac{dN_f}{ds}(s)(t-s)^{m-1}\, ds = \alpha_1, \tag{14.10}$$

$$\frac{d\alpha_1}{dt} = m\,(m-1) C_m\, G^m \int_0^t \frac{dN_f}{ds}(s)(t-s)^{m-2}\, ds = \alpha_2, \tag{14.11}$$

$$\frac{d\alpha_2}{dt} = m\,(m-1)(m-2)\, C_m\, G^m \int_0^t \frac{dN_f}{ds}(s)(t-s)^{m-3}\, ds = \alpha_3, \tag{14.12}$$

etc., which, for integer values of m, terminate and provide a useful way for investigating various forms of the flow-induced crystallization by simply specifying the flow-induced nucleation rate, as shown below.

Equations (14.9)–(14.12) are also valid for quiescent crystallization if the flow-induced nucleation rate and crystalline fraction that appear in these equations are replaced by the thermal nucleation rate and crystalline fraction, respectively.

14.2.2 Nakamura's Crystallization Kinetics

For quiescent variable temperature conditions, Nakamura et al. (1972) proposed the following expression for the (relative) crystalline fraction

$$\alpha = 1 - \exp\Big(- \int_0^t K_N ds\Big)^n, \tag{14.13}$$

where K_N depends on the temperature and flow conditions.

For constant K_N, (14.13) reduces to the well-known Avrami-Kolmogorov's kinetics. In the quiescent state, $m + 1 = n$, but Nakamura's expression does not have a strong physical support (Eder and Janeschitz-Kriegl 1997; Eder et al. 1990).

14.2.3 Ziabicki's Model

Instead of describing the kinetics of phase transformation/crystallization with complicated mathematical models, Ziabicki (1974, 1976) proposed to model it by means of the following first-order ordinary differential equation

$$\frac{d\alpha}{dt} = K(T)(1 - \alpha(t)), \tag{14.14}$$

where $K\,(T)$ is a temperature-dependent crystallization rate function.

According to (14.14), for isothermal processes, the crystallinity is an exponential function of time, while, for non-isothermal ones, the crystallization rate function depends on the cooling rate. Because of its simplicity, Ziabicki's model (1974,

1976) has also been used to account for flow-induced crystallization by considering that the crystallization rate function depends on both the temperature and the molecular orientation, as discussed below.

14.2.4 Schneider's Model of Quiescent Crystallization

For non-isothermal conditions, the crystal volumetric fraction of each phase $\phi_i\,(t)$ may be modelled through Schneider's formulation (Schneider et al. 1988), i.e.,

$$\frac{d\phi_3}{dt} = 8\pi\frac{dN}{dt}, \tag{14.15}$$

$$\frac{d\phi_2}{dt} = G\phi_3, \tag{14.16}$$

$$\frac{d\phi_1}{dt} = G\phi_2, \tag{14.17}$$

$$\frac{d\phi_0}{dt} = G\phi_1, \tag{14.18}$$

where $\phi_3 = 8\pi N, \phi_2 = 8\,\pi\,R_t, \phi_1 = S_t, \phi_0 = V_t, \frac{dN}{dt}$ and G are the nucleation and growth rates, respectively, V_t and S_t are the total volume and surface of the spherulites, respectively, N is the number of nuclei and R_t denotes the sum of the radii of the spherulites. Note that (14.15)–(14.18) are closely related to (14.10)–(14.12).

The nucleation density N and the growth rate of each phase G_i are functions of pressure p and temperature T as, for example,

$$N(p,T) = N_r\exp\big(-c_n\,(T(t) - T_{Nr}\,(p))\big), \tag{14.19}$$

$$G_i(p,T) = G_{i,max}\exp\big(-c_{gi}\,\big(T(t) - T_{Gi}(p)\big)^2\big)\,, \tag{14.20}$$

where N_r and $G_{i,max}$ are (constant) reference values, T_{Nr} and T_{Gi} are the (constant) reference temperatures corresponding to N_r and $G_{i,max}$, respectively, and c_n and c_{gi} are assumed to be constant.

During solidification in a multiphase system, every crystal from phase i generates a crystal volume fraction ϕ_{0i} using a share of the available number of nuclei and its own growth rate. Since the ratios in which the nuclei are divided between the crystal phases is not known, it may be assumed that the allocation of nuclei to a crystal phase scales with the ratio of the individual crystal growth rates at the current pressure and temperature conditions. This means that, for isobaric conditions, the nucleation rate of phase i is given by

$$\frac{dN_i}{dt} = g_i \frac{dN}{dt} \frac{dT}{dt}, \tag{14.21}$$

where $g_i = G_i(t)/\sum G_i(t)$ is the growth rate fraction and the summation is over the number of phases. This model can be generalized to account for the presence of polymorphs by including the presence of nucleation agents (van Drongelen et al. 1988).

14.2.5 Zuidema's Model of Flow-Induced Crystallization

In order to account for flow-induced nucleation and crystallization, Zuidema (Zuidema 2000; Zuidema et al. 2001; Peters 2003) proposed a modification of the shear-induced crystallization model proposed by Eder and Janeschitz-Kriegl (1997) and Eder et al. (1990) which provides a good correlation between the predicted flow-induced structures and experimental data.

Zuidema's model employs a recoverable strain model with a Leonov's driving force (Leonov 1976, 1987) for flow-induced crystallization that correlates most strongly with the viscoelastic mode associated with the largest relaxation time. Zuidema only accounted for the second invariant of the deviatoric part of the recoverable strain rate tensor which is a measure of the molecular orientation, but no model for the molecular orientation was included in his flow-induced crystallization formulation.

Zuidema's modification of Schneider's model (Schneider et al. 1988) can describe the non-isothermal crystallization of cylindrical structures sometimes referred to as shish-kebabs and may be written as

$$\frac{d\varphi_3}{dt} + \frac{\varphi_3}{\tau_n} = 8\,\pi J_2 g_n, \tag{14.22}$$

$$\frac{d\varphi_2}{dt} + \frac{\varphi_2}{\tau_l} = J_2 \varphi_3 \frac{g_l}{g_n}, \tag{14.23}$$

$$\frac{d\varphi_1}{dt} = G\varphi_2, \tag{14.24}$$

$$\frac{d\varphi_0}{dt} = G\varphi_1, \tag{14.25}$$

$$\varphi_0(t) = -\ln(1-\alpha(t)), \tag{14.26}$$

where $\varphi_2 = 4\,\pi L_l$, J_2 is the driving force, the scaling factors g_n and g_l describe the sensitivity of the flow-induced nuclei and length L to J_2, respectively, and τ_n and τ_l are the relaxation times associated with the nuclei and length, respectively.

If nucleation is considered as acting as a cross-link, an increase in the number of nuclei causes an increase in the rheological relaxation time. The simplest of such a relation is a linear one.

It must be noted that in the presence of flow, both spherulites and flow-induced structures contribute to the degree of space filling, and the Avrami-Kolmogorov's impingement model is then described by (cf. (14.3))

$$\phi_0\,(t) + \varphi_0\,(t) = -\ln(1-\alpha(t)). \tag{14.27}$$

It should also be noted that the time derivatives that appear in (14.14), (14.15)–(14.18) and (14.22)–(14.25) must be replaced by material derivatives, e.g., $\frac{D\phi}{Dt} \equiv \frac{\partial\phi}{\partial t} + \boldsymbol{v}\cdot\nabla\phi$, where $\boldsymbol{v}$ is the velocity vector for the crystal phase. If the amorphous and crystalline phases are considered as a homogeneous fluid, then the velocity $\boldsymbol{v}$ coincides with that of the mixture. The use of a material derivative implies that (14.14), (14.15)–(14.18) and (14.22)–(14.25) are hyperbolic with characteristic lines whose slopes coincide with the components of $\boldsymbol{v}$ (Zachmanoglou and Thoe 1986) and only require an initial condition and one boundary condition in each coordinate direction.

For steady, uniaxial flows, the solution of (14.14) is

$$\alpha = 1 - C\exp\left(-\int_0^x \frac{K(T(s))}{u(s)}ds\right), \tag{14.28}$$

which indicates that the crystalline fraction depends on the histories of both the axial velocity component and the fiber's temperature. In (14.28), x is the distance along the fiber measured from the die's exit, and C is a constant that may be determined from the crystalline fraction at $x=0$. If the crystalline fraction at the die's exit is nil, $C=1$, and a comparison of (14.28) with (14.3) indicates that $\alpha_{af} = \int_0^x \frac{K(T(s))}{u(s)}ds$, for Ziabicki's model.

For the Schneider's and Zuidema's crystallization models discussed above, one may obtain an expression for the crystalline fraction for steady, uniaxial flows as for the Ziabicki's model by first integrating, for example, (14.22) to obtain φ_3 as a function of J_2. and g_n, then integrating (14.23) to obtain φ_2 as a function of to obtain φ_3, then integrating (14.24) to obtain φ_1 as a function of to obtain φ_2, then integrating (14.25) to obtain φ_0 as a function of to obtain φ_1, and finally substituting the value of φ_0 thus obtained in (14.26) which may be written as $\alpha = 1 - \exp(-\varphi_0\,(t))$.

The integrals mentioned in the previous may be performed easily by first introducing a new time-like variable τ defined $\tau = \int_0^x \frac{1}{u(s)}ds$, which corresponds to the fluid residence time, and may be performed analytically if the relaxation times associated with the nuclei and length of the crystals are assumed to be constant. Under such conditions, it can be easily deduced that the crystalline

fraction depends on the driving force J_2, the scaling factors g_l and g_n, and the growth rate G. Furthermore, these factors appear as integrals which correspond to the particular solutions of (14.22)–(14.25) and, therefore, the crystalline fraction includes their history from the die's exit.

14.2.6 Eder and Janeschitz-Kriegl's Model of Flow-Induced Crystallization

Eder and Janeschitz-Kriegl's model corresponds to replacing J_2 in (14.22) by the square of the nondimensional shear rate (Eder and Janeschitz-Kriegl 1997; Eder et al. 1990; Eder 1997). Therefore, Eder and Janeschitz-Kriegl's model of flow-induced crystallization accounts for the strain-rate enhancement of crystallization.

14.2.7 Other Models of Flow-Induced Crystallization

Other authors have proposed models of flow-induced crystallization based on the strain rate tensor (Keller and Kolnaar 1998), normal stress difference (Ziabicki et al. 2013), trace of the stress tensor (Doufas et al. 1999, 2000a), changes in the dumbbell free energy induced by the flow (Zheng and Kennedy 2004), work-input (Janeschitz-Kriegl 2003), recoverable strain (Zuidema 2000; Zuidema et al. 2001; Peters 2003), configurational entropy of polymer chains (van Meerveld 2005; van Meerveld et al. 2008), suspension theory (Tanner 2002, 2003), microrheological approximations (Coppola et al. 2001, 2004), rational thermodynamics (Rao and Rajagopal 2002a, b), matrix or network methods (Flory 1947), GENERIC (Hütter 2004; Hütter et al. 2003), etc.

In the next paragraphs, some of the models mentioned above are described in some detail. Further crystallization models have been reviewed by Di Lorenzo and Silvestre (1999), Long et al. (1995), Strobl (2006), Fukuda et al. (2004), Schultz (2001), and Piorkowska et al. (2006).

The continuum model introduced by Doufas et al. (1999, 2000a) is a macroscopic one that combines irreversible thermodynamics through the continuum Hamiltonian/Poisson bracket formalism with the Avrami-Kolmogorov kinetic equation for polymer crystallization. Since it is a continuum model, the details of the molecular mechanisms involved in either flow-induced crystallization or the crystal morphology are not taken into consideration, and, therefore, only the macroscopic characteristics of the overall crystallization kinetics and the rheological behavior of semicrystalline polymers are considered.

In Doufas et al.'s model, both the amorphous and crystalline phases are accounted for; a modified Giesekus fluid (Giesekus 1982) is used for the rheology of the amorphous phase, while the crystalline phase is modeled as a collection of

multibead rigid rods that grow and orient in the flow field. The model also includes evolution equations for the conformation tensor, orientation tensor and degree of crystallinity, and reduces to the modified Giesekus model for the melt and the quiescent Avrami's kinetics in the absence of flow. In addition, it contains only two adjustable parameters related to the relaxation time of the crystalline phase and the coupling between the amorphous and crystalline phases.

Flow-induced crystallization models based on suspension theory (Tanner 2002, 2003) consider a system of rigid spheres (crystallites) embedded in a fluid matrix which may follow a Newtonian (Tanner 2002) or a linear viscoelastic rheology (Tanner 2003); the latter is only valid for small strains. However, the model may be generalized and the amorphous phase may be treated as a PTT (Phan-Thien-Tanner) or General Network model.

One of the main problems of the Doufas et al. (1999, 2000a) continuum and the suspension theory models (Tanner 2002, 2003) is the treatment of the total stress as crystals are formed. A simple approach assumes that the stresses of the amorphous and crystalline phases are additive, i.e., as the crystallization progresses, rigid spheres are introduced into the amorphous matrix. Such an approach, however, implies the presence of a mixture of the crystalline and amorphous phases at each point, whereas microscopic observations show the presence of distinct macroscopic crystallites in an amorphous matrix. A remedy to this problem is to assume that the contributions of the amorphous and crystalline phases to the total stresses is weighted by the crystalline fraction, even though the stresses are surface forces per unit area and the crystalline fraction refers to volume.

The dumbbell model proposed by Zheng and Kennedy (2004) is similar to those of Doufas et al. (1999) and Tanner (2002) in that the crystallizing system is considered as a suspension of semicrystalline entities growing in an amorphous matrix. However, in Zheng and Kennedy's model, the physical properties of the amorphous phase are assumed to be constant, so that the physical properties of the suspension depend only on the semicrystalline phase.

In order to describe the chain conformation and orientation evolution of the amorphous phase, Zheng and Kennedy (2004) employed the FENE-P (Finite Extensible Nonlinear Elastic model with a Peterlin closure approximation) dumbbell model, whereas the semicrystalline phase was modeled as a collection of rigid dumbbells, and the contribution of the amorphous and crystalline phases to the total stress was assumed to be additive.

The flow-induced crystallization model developed by Coppola et al. (2001, 2004) is microrheological, i.e., the polymeric liquid is described on a molecular basis, the flow is considered to increase the nucleation rate by increasing the free energy of the liquid phase, and the nucleation rate follows the formulation proposed by Lauritzen and Hoffman (1960, 1973) that accounts for the volumetric free energy difference between the liquid and crystalline phases, the activation energy of the supercooled liquid nucleus interface, and energetic and geometrical factors for the crystalline nuclei (Hoffman and Miller 1997).

Coppola et al. (2004) have shown that, for isotactic polypropylene, as the temperature decreases, the corresponding increase in chain orientation at a given

shear rate leads to a faster crystallization; their model is based on Doi-Edwards' microrheological theory (Doi and Edwards 1986).

The thermodynamic approximation proposed by Rao and Rajagopal (2002a, b) for determining the flow-induced crystallization is based on the formulation of constitutive equations that involve the concept of multiple natural configurations and obtains evolution equations for the natural configuration and mass fraction of the crystalline material by maximizing a prescribed rate of dissipation. This approach combines continuum mechanics and thermodynamics, assumes that effects are additive, and results in different models that depend on the forms used for the internal energy, entropy and dissipation rate.

The network model for modeling flow-induced crystallization is based on an extension of the work of Flory (1947) on the stress-induced crystallization of rubber. Such an extension assumes that temporary network junctions play the same role as the chemical cross-links in the theory of rubber crystallization, and is based on the decrease in entropy associated with the stretching of the molecular chains and the tendency of the polymer to crystallize.

In the *configurational entropy flow*-induced *crystallization model*, the rheology of the polymer melt is described by a thermodynamically consistent reptation model developed by Öttinger (1999) for monodisperse entangled linear polymer systems and extended to polydisperse systems by van Meerveld (2005). The thermodynamically consistent reptation model is a variation of the Doi-Edwards "tube" and reptation model (Doi and Edwards 1986) that incorporates the convective constraint release (CCR) mechanism proposed by Marrucci (1996) which takes into account how the removal of tube segments (which represent entanglements) influences the relaxation of the contour path, whereas the CCR mechanism accounts for the number of constraints lost due to the retraction of the chains forming the tube.

The thermodynamically consistent reptation model approach is mainly based on molecular theory and describes the evolution of the polymer chain contour path by a configuration distribution function *which depends on* the unit orientation vector and the curvilinear coordinate associated with the position of polymer segments along the contour path. Such a function is given by a Fokker-Planck equation for a monodisperse sample.

The thermodynamically consistent reptation model may be incorporated into a non-equilibrium thermodynamic GENERIC (General Equation for Non-Equilibrium Reversible Irreversible Coupling) framework (Öttinger 1999). Such a model includes a set of rate equations for the nucleation and growth stages, where the governing parameter for nucleation is the change in the configuration of amorphous chains, and pays special attention to the high molecular tail of the molecular weight distribution function, since this part of the distribution function contributes most to flow-induced crystallization.

In the thermodynamically consistent reptation model, flow-induced crystallization is assumed to occur only when the reduction of the end-to-end distance of the amorphous part of the chain is large compared to the increase of the relative extension of the chain under flow (van Meerveld 2005; van Meerveld

et al. 2008). Consequently, the onset of orientation and stretching is characterized by means of Deborah numbers based on the reptation and stretching times of the high molecular weight chains.

It must be pointed out that the models of flow-induced crystallization that make use of the stress tensor, normal stress difference and configurational entropy have been mainly developed for melt-spinning processes.

14.2.8 Comparisons of Models for Flow-Induced Crystallization

The flow-induced crystallization models described above represent quite well the current state of the subject, but they are certainly not exclusive and there are more models not included here. As noted above, many of these models are based on the Avrami-Kolmogorov equation which was modified to account for enhanced crystallization due to the flow by introducing an orientation factor (Ziabicki 1976) which depends on the flow, as described in Sect. 14.5.

In deciding the applicability of a crystallization model to a particular situation, e.g., fiber spinning, one must take into consideration that flow-induced crystallization may depend on the shear rate, strain rate, stress, normal stress difference, recoverable shear strain, free energy of dumbbells, rheology, configurational entropy of the polymer chains, work input, etc., and that the factor that exerts the greatest influence on crystallization and under what conditions does so is as yet subject to debate. Moreover, some of the models have been developed mainly for isothermal conditions, e.g., (Doufas et al. 1999, 2000a), whereas others, e.g., (Eder and Janeschitz-Kriegl 1997; Eder et al. 1990), may be applied to non-isothermal processes. Furthermore, since the rheology of the polymer should take into account the molecular motion of the polymer chains which is affected by the crystallization and the latter is in turn affected by the rheology, the choice of viscoelastic rheology such as the Leonov's recoverable stress, pom-pom, extended pom-pom (XPP), PTT, etc., determines to a large extent the quality of the flow-induced crystallization model. This is the case for the Zuidema (Zuidema 2000; Zuidema et al. 2001; Peters 2003), Tanner (Tanner 2002, 2003), microrheological (Coppola et al. 2001, 2004) and Zheng and Kennedy (2004) flow-induced approximations. On the other hand, other models such as those of Eder and Janeschitz-Kriegl (Eder and Janeschitz-Kriegl 1997; Eder et al. 1990) and Doufas et al. (1999, 2000a) are based on global behavior such as the one observed in rheological and rheological-optical experiments.

Many of the flow-induced crystallization models developed to-date are based on experimental data for a small sample of polymers, e.g., PP, PE, i-PP, etc., for which the material properties are available. However, these polymers have properties that are quite different from those of other polymers and, for example, the suspension assumption used for certain polymers, e.g., PP, may not be applicable to other

polymers (Tanner and Qi 2005). This means that any flow-induced crystallization model should be tested for a wide range of materials.

The experimental methods on which a flow-induced crystallization model is based or tested are also important to decide for which specific type of flow, e.g., elongational or shear flow, and conditions, e.g., post-flow or continuous flow, the model can be applied. For example, the Doufas et al. (1999, 2000a) model was developed for fiber spinning, while those of Eder and Janeschitz-Kriegl (1997) and Zheng and Kennedy (2004) were aimed at modeling injection molding, i.e., post-shearing conditions.

Although some models have been claimed to be suitable for both shear and elongation flows, e.g., (Zuidema 2000; Zuidema et al. 2001; Peters 2003), their applicability remains still an issue due to the lack of data for elongation-induced crystallization.

14.3 Models for Molecular Orientation

The properties of liquid crystalline polymers depend strongly on their molecular orientation; a high degree of orientation results in high strength and stiffness along the alignment direction, but it also yields anisotropic properties that may be detrimental when multidimensional stability and strength are required (Ramalingam and Armstrong 1993).

The relationship among the flow, molecular orientation, crystallization and rheology of LCP is a complex one, and depends on many factors. For isothermal flows at low shear rates, a nematic LCP may be called flow-aligning because shear promotes the alignment of the nematic director at an angle with respect to the flow direction, but shear may also result in tumbling which is characterized by a continuous rotation of the director. Although considerable progress has been made in the molecular orientation of lyotropic solutions of rodlike polymers, the situation is not yet as advanced in the case of thermotropic LCP.

Orientation of chain segments within a deformed chain leads to another important effect. Chain segments with orientations prevailing in the system, e.g., segments parallel to the filament axis in melt-spinning, crystallize at higher temperatures and at higher rates than segments with less frequent orientations. This leads to the preferential formation of axially oriented crystals and discrimination of crystals with orientations perpendicular to the main axis.

Experimental evidence about selective crystallization is scarce and indirect, although this concept is supported by comparisons of the crystal and amorphous orientation factors in crystallization experiments performed under stress or flow. Moreover, deformation of the polymer chains leads to a reduction of the configurational entropy, an elevation of melting temperature, and an increase of both the nucleation and the crystallization rates; the crystallization characteristics can also be affected by stress as discussed previously.

In order to predict the flow alignment of nematic polymers, molecular, mesoscopic and continuum models have been developed. The objective of these theories is to predict the most probable direction of alignment and the spreading of the orientation distribution in terms of a few parameters.

The Leslie-Ericksen continuum formulation (Leslie 1968, 1979; Ericksen 1960, 1991) provides explicit expressions for the flow alignment as a function of the Miesowicz viscosities independently of the shear rate, but it provides no information on the spread of the orientation distribution. In addition, this formulation does not contain any information on the concentration and is only applicable to small molecular weight liquids, i.e., liquid crystals. Furthermore, in this approach, the stress tensor is assumed to have a linear dependence on the strain rate tensor and the angular velocity of the director, and implicitly assumes that the characteristic time associated with the deformation is much larger than the characteristic relaxation time of the nematic phase. This explains, in part, the success of the Leslie-Ericksen formulation for low molecular-weight crystals because their relaxation times are usually much smaller than the macroscopic time scales. In fiber spinning, however, the deformation rate is usually much larger than the inverse of the relaxation times and, therefore, the Leslie-Ericksen theory becomes inapplicable.

High-molecular weight polymers and LCP exhibit many relaxation times which are associated with the relaxation of the short and long parts of the molecular chains; the largest relaxation time is related to the relaxation of the chain as a whole and may dominate its macroscopic behavior. This justifies that, in some cases, one may use only the longest relaxation time instead of the whole spectrum of relaxation times such as, for example, in the Rouse model for unentangled polymer liquids (Rouse 1953; Long and Morse 2002; Lin 2010) or the reptation model for entangled ones. In LCP solutions, the persistence length of the molecular chains is not negligible compared with their contour one and this leads to an anisotropic equilibrium state and a dependence of the molecular distribution function on the nematic order parameter.

Mesoscopic models have been developed to predict shear-aligned steady states and are able to predict the dependence of the Leslie angle on the concentration and the molecular aspect ratio, but require either direct numerical simulations or a higher-order asymptotic analysis to obtain the dependence of the molecular orientation on the shear rate (Wang 1997; Rienacker and Hess 1999; Forest and Wang 2003; Forest et al. 2003; Maffetone et al. 2000; Cocchini et al. 1990).

Approaches based on kinetic theory employ an evolution equation for the probability density function and should include the dependence of the molecular orientation upon the properties of the polymer and flow, e.g., shear. However, it is difficult to obtain explicit expressions for such a dependency.

Kinetic approaches are mainly based on the work of Onsager (Onsager 1949) and, although much progress has been made since, few analytical works have appeared on the subject, except for that of Marrucci and co-workers (Marrucci and Maffetone 1989; Marrucci 1991; Maffetone et al. 1994) who provided an explanation of the dependence of the molecular orientation on the normal stress difference. This is not surprising at all, for numerical simulations indicate that the

shear-perturbed nematic equilibrium contains many high-order spherical harmonics, and it is nearly impossible to obtain a distribution function that resolves them. In addition, it is well-known that nematic polymers exhibit multiple stable phases, e.g., an isotropic phase for dilute concentrations, a nematic phase at high concentrations, and bistability in an overlap region (de Gennes 1974).

The isotropic phase can be treated easily by means of kinetic theory and mesoscopic approaches in the weak-shear limit and for dilute concentrations by means of asymptotic methods. Such approaches provide explicit expressions for the alignment angle, degree of alignment and normal and shear stresses as functions of the molecular parameters and the shear rate.

Many of the models used to predict molecular orientation in fiber spinning processes of liquid crystalline polymers are based on a kinetic equation for the probability density function $f(\boldsymbol{u},t)$ that provides the probability that a dumbell or (rigid) rod-like polymer be in the direction $\boldsymbol{u}$ at time t. For polymers in a Newtonian solvent subject to anisotropic hydrodynamic drag, Bhave et al. (1993) used a polymer-polymer mean-field interaction approximation with a Maier-Saupe potential (Maier and Saupe 1958, 1959, 1960), generalized the results of Doi (1980, 1981) and Doi and Edwards (1986) and introduced a closure approximation whereby the fourth-order moments of the probability function for $\boldsymbol{u}$ are approximated by products of second-order ones. In this manner, they obtained an approximate equation which couples the structure/orientation/order tensor to the Navier-Stokes equations. This approximation indicates that the deviatoric stress tensor becomes the sum of two terms; the first one is given by the classical Newtonian rheology, whereas the second one depends on the temperature, the structure tensor $\boldsymbol{Q}$, the velocity gradient tensor, and a parameter that characterizes the strength of the intermolecular Maier-Saupe potential which is responsible for orienting the molecules in the same direction.

The nematic structure tensor is traceless, is symmetric, has three real eigenvalues, and can be diagonalized. For uniaxial nematic liquid crystals, two eigenvalues are identical, and the eigenvector corresponding to the third eigenvalue provides the distinguished orientation direction and admits a representation in terms of a scalar order parameter that is related to the polymer direction vector $\boldsymbol{u}$. This scalar parameter s can be interpreted as the average degree of orientation between the polymer molecular direction vector $\boldsymbol{u}$ and the direction of the third eigenvector of the structure tensor. The values $s=0$ and 1 correspond to an isotropic state referred to as a nematic defect since the structure tensor is nil; these values also correspond to no preferred orientation and parallel alignment of the third eigenvector and $\boldsymbol{u}$, respectively. On the other hand, $s=-0.5$ corresponds to all molecules being aligned in a plane orthogonal to the third eigenvector of the structure tensor; $0<s\leq 1$ and $-0.5\leq s<0$ correspond to liquid crystals that exhibit prolate and oblate, respectively, uniaxial symmetry. On the other hand, if all the eigenvalues of the structure tensor are distinct, the order tensor depends on five parameters due to its being traceless, and admits a biaxial representation that depends on two parameters that are related to the degree of orientation of the

molecular direction vector $\boldsymbol{u}$ and the second and third eigenvalues of the structure tensor.

In their studies of isothermal spinning of nematic liquid crystal polymers, Ramalingam and Armstrong (1993) used the constitutive equations of Bhave et al. (1993), and assumed uniaxial symmetry and that the direction of the third eigenvector of the orientation tensor coincides with the elongational direction. This implies that the principal direction of the structure tensor also referred to as the axis of symmetry of the structure tensor coincides with the symmetry axis of the fiber and is uniform throughout the fiber, and, therefore, the structure tensor can be characterized by only a scalar order parameter which indicates the degree of orientation of the dumbbell direction $\boldsymbol{u}$ with respect to the fiber's symmetry axis. A similar study was reported by See et al. (1990).

Ramalingam and Armstrong (1993) also showed that, in contrast, with fiber spinning processes of isotropic liquids, the velocity, structure and stress profiles are sensitive to the choice of initial conditions.

In a nonequilibrium elongational flow, the structure tensor is not uniformly uniaxial and the third eigenvector of the orientation tensor may not coincide with that of the fiber's symmetry axis because the strain rate tensor is not diagonal; in such a case, the uniaxial symmetry is broken. However, for slender fibers, one may consider that a uniaxial flow approximation is approximately valid and, therefore, the structure tensor may be assumed to be nearly uniaxial. This can be justified asymptotically by means of perturbation methods for slender fibers at low Reynolds numbers where the small perturbation parameter is the slenderness ratio (Ramos 1999).

Other kinetic approaches are based on the Smoluchowski equation for the orientational probability density function (Forest et al. 2002, 2004). These approaches have been developed for dilute concentrations under weak shear to analyze isotropic-to-nematic phase transitions and also make use of the Doi's formulation (Doi 1980, 1981; Doi and Edwards 1986).

The Doi's formulation (Doi and Edwards 1986) with the Maier-Saupe potential (Maier and Saupe 1958, 1959, 1960) has also been used to analyze the microstructure in one-dimensional isothermal models of slender liquid crystalline polymer fibers (Forest et al. 1997a) and to determine the effects of the coupling between the flow and the molecular orientation on the linear stability of isothermal LCP fibers (Forest et al. 1997b).

Doi's approach has also been used to developed one-dimensional models of thermotropic liquid crystalline fibers (Zhou et al. 2000) by including the energy equation, axial conduction and heat transfer losses through the fiber's surface and a temperature dependence of the relaxation time that appears in the orientation/structure tensor which, in turn, affects the deviatoric stress tensor. It has also been extended to study fiber spinning of liquid semi-crystalline, compound (Ramos 1999, 2002, 2006, 2007), hollow-compound (Ramos 2001a, 2005a) and annular fibers (Ramos 2001b).

In Zhou et al.'s model (2000), the total stress tensor was assumed to be the sum of an isotropic Newtonian contribution and an anisotropic part that depends on the

temperature, velocity gradient and structure tensor. The isotropic contribution of the Newtonian stress tensor was assumed to obey a Newtonian rheology with a dynamic viscosity that depends in an Arrhenius manner on the temperature. Although the authors refer to their model as a two-phase one, this is not strictly so, for they do not account in a separate form for the evolution of the amorphous and crystalline phases. Moreover, whenever the fiber solidifies, their one-dimensional model predicts a constant velocity along the fiber, but the evolution equation for the scalar order parameter of the molecular orientation may predict the unphysical result that the molecular orientation decreases once solidification occurs due to the fact that the uniaxial bulk free energy that is based on the Maier-Saupe intermolecular potential, may dominate over the elongational terms that appear in that equation. This non-physical behavior is observed in their results and may be eliminated entirely by modifying the Maier-Saupe potential when the scalar order parameter for the molecular orientation is close to its maximum value, i.e., unity.

As indicated above, in the mean-field Maier-Saupe theory, the structure tensor order parameter is defined in terms of the second-order moments of the probability density function; this imposes certain constraints on the eigenvalues of the structure tensor that may be interpreted as constraints. By way of contrast, in the Landau-de Gennes energy functional framework (de Gennes 1974), the order parameter of the structure tensor is often defined independently of the probability density function, and the theory makes physically unrealistic predictions about the equilibrium order parameter in the low-temperature regime.

Ball and Majumdar (2010) have developed a continuum energy functional that interpolates between the mean-field Maier-Saupe energy and the Landau-de Gennes energy functional by defining a thermotropic bulk potential that blows up whenever the eigenvalues of the structure tensor reach physically unrealistic values and, as a consequence, the minimizers of their continuum energy functional yield physically realistic order parameters in all temperature regimes.

One of the most challenging problems in polymer science is the reliable prediction of molecular orientation during crystallization; the viscoelastic nature of polymers should be accounted for in the description of the evolution of the molecular orientation and vice versa. The alignment of macromolecules along a preferred direction is the result of a competition between the polymer's relaxation times which are functions of the thermochemical and crystallization histories, and the characteristic deformation time; high alignment is expected when the ratio of the latter to the former is greater than unity.

14.4 Rheology

Both molecular orientation and crystallization have a strong effect on the melt rheology; in many cases, the solidification of a semi-crystalline material is caused by crystallization rather than by temperature. Despite its importance, the effects of

the crystallinity on the polymer's rheology, e.g., viscosity, have not been treated with sufficient detail and the literature on this subject is scarce. This may be due to difficulties in measuring simultaneously the rheological properties and the crystallinity evolution.

Most researchers agree that the melt viscosity experiences a dramatic increase in viscosity when the degree of crystallization reaches a critical value which may not coincide with the ultimate degree of crystallization.

Models for the dependence of the dynamic viscosity on the crystallinity include polynomial, exponential, and rational ones (Pantani et al. 2005; Ziabicki and Jarecki 2007); in polynomial models, for example, the dynamic viscosity is given as a polynomial of the crystallinity degree. Both polynomial and exponential models provide analytical expressions for the melt viscosity which increases in a smooth manner with the degree of crystallization. By way of contrast, rational models (Ziabicki and Jarecki 2007) are not analytical ones and the dynamic viscosity becomes unbounded at the critical value of the degree of crystallization; this behavior may cause a great deal of problems when implemented numerically.

The dependence of the dynamic viscosity on the temperature has been usually assumed to follow an Arrhenius expression; a similar expression has also been assumed for the dependence of the relaxation times which should also depend on the molecular orientation and crystallization, although it is difficult to measure such a dependency experimentally.

As discussed previously the contributions of the amorphous and semicrystalline phases to the total deviatoric stress tensor are usually assumed to be additive or weighted by the crystallization degree. Such a simple assumption may not be physically consistent due to the interactions between the amorphous and crystalline phases which include both tangential and normal effects along the amorphous-crystalline interfaces, and may not satisfy the principles of rational mechanics and thermodynamics.

14.5 Models of Fiber Spinning Processes

Most models of fiber spinning of liquid semi-crystalline polymers developed to-date are one-dimensional. The first one-dimensional model was perhaps developed by Matovich and Pearson (1969) for amorphous or isotropic polymer melts and was based on a heuristic derivation based on a control-volume formulation where the flow was assumed to be mainly one-dimensional; such an assumption is valid for slender fibers, i.e., fibers characterized by a maximum diameter-to-length ratio much smaller than unity. In addition, the model developed by Matovich and Pearson was isothermal and employed a Newtonian rheology, although later developments have included isotropic viscoelastic rheologies (Denn et al. 1975; Betchel et al. 1988, 1995) and thermal effects (Glicksman 1968; Hyunh and Tanner 1983; Kase and Matsuo 1965; Ziabicki 1976; Pearson 1985; Vassilatos et al. 1992; Gagon and Denn 2004).

The model developed by Matovich and Pearson (1969) can also be derived by expanding the flow variables in Taylor's series expansions of the radial coordinate measured from the fiber axis and truncating the resulting series at different orders in that coordinate (Vrentas and Vrentas 2004). It may be shown that the Matovich and Pearson's model corresponds to retaining only the first two terms in the Taylor series expansions and results to this order in an axial velocity component which only depends on the distance along the fiber, while the radial velocity component is a linear function of the radial coordinate. Maintaining higher-order terms in the Taylor's series expansions results in more equations for the coefficients of such expansions and accounts for the radial dependence of the flow variables. However, the validity of a truncated series expansion model can only be justified for slender fibers, i.e., fibers whose largest diameter is smaller than the distance from the location of largest fiber's cross-section to the take-up drum, and small Reynolds numbers.

A different approximation for obtaining one-dimensional models consists in nondimensionalizing the governing equations for the conservation of mass, linear momentum and energy, introducing the slenderness ratio as a small parameter, expanding the flow variables in asymptotic power series of the slenderness ratio, i.e., using a long-wave or lubrication approximation, and equating to zero the coefficients that multiply the same power of the slenderness ratio (Schultz and Davis 1982). Asymptotic methods based on the slenderness ratio have also been used to study melt spinning of compound (Ramos 1999, 2002, 2006, 2007), hollow-compound (Ramos 2001a, 2005a) and annular fibers (Ramos 2001b).

To first-order in the slenderness ratio and for low Reynolds numbers, the Matovich and Pearson's model results, whereas higher-order approximations provide corrections to the leading-order one and include the radial dependence of the flow variables. This asymptotic procedure indicates that, at leading-order in the expansion, the temperature across the fiber is uniform and this in turn implies that the Biot number which is a measure of the convective heat exchanges of the fiber with its surroundings relative to thermal conduction in the fiber must be small and this, in turn, implies that, at leading-order in the slenderness ratio, the outer surface of the fiber is adiabatic (Ramos 2005a, 2006, 2007). Such a restriction does not appear explicitly in the control-volume formulation approach employed by Matovich and Pearson (1969) but it is a realistic one because, in modern spinlines, the temperature is maintained high enough in order to delay solidification and, therefore, allow the molecular orientation, elongational flow and heat conduction in the axial direction to interact with each other long enough along the fiber.

Asymptotic methods based on the slenderness ratio are not appropriate when there is rapid surface cooling due to the large radial temperatures present under these conditions, and the validity of one-dimensional models based on control-volume formulations may not be justified in the presence of rapid surface cooling because of the strong radial temperature gradients generated at the fiber's outer radius or free surface.

A third method for deriving one-dimensional models of fiber spinning processes consist of using the integral forms of the governing equations for mass, linear

momentum and energy conservation across the fiber, integrating analytically the terms which contain the radial derivatives and approximating the integral terms across the fiber by functions that only depend on the axial coordinate along the fiber; alternatively, the flow variables may be expanded in Taylor's series expansions of the radius and the above-referred-to integrals may be performed analytically. In any event, only a finite number of terms of the Taylor's series expansion is kept and, therefore, the resulting equations are truncated at some order on the fiber's outer radius.

14.5.1 One-Dimensional Models for Fiber Spinning of Liquid Semi-Crystalline Polymers

The available one-dimensional models for fiber spinning of liquid crystalline and liquid semi-crystalline polymers may be derived by means of the same methods described above for amorphous or isotropic materials, and may be classified in two main groups: one- and two-phase models depending on whether the amorphous and semi-crystalline phases are considered as a single material or two different materials, respectively. One- and two-phase models may in turn be classified according to the rheologies employed for each phase and may be isothermal and non-isothermal.

In the next sections, a brief review of the main one-dimensional models for fiber spinning of liquid semi-crystalline polymers developed to-date is presented.

14.5.1.1 One-Phase Models

The main one-phase models for the spinning of liquid crystalline and liquid semi-crystalline fibers developed to-date include those of van Meerveld (van Meerveld et al. 2008) that employs Schneider's model for quiescent crystallization, i.e., nucleation and growth of three-dimensional spherulites, and a model for the fibrillar morphology development due to flow-induced nucleation and longitudinal growth of the fibrillar structures. It also includes a Newtonian rheology where the dynamic viscosity is an exponential function of the degree of crystallization and temperature that models the influence of the crystallization on the rheological behavior, while the amorphous phase is described by a microrheological model based on a configuration tensor that includes an upper-convective Maxwell behavior for the change of the configuration tensor with the flow, a Giesekus mobility matrix for the relaxation dynamics, finite extensibility of the polymer chains, and the reduction of configuration due to crystallization. The model contains a large number of constants that must be determined by judicious comparisons between its predictions and experimental data. The model is able to predict the neck-in phenomenon which may be observed at high drawing speeds.

The model developed by Zuidema and co-workers (Zuidema 2000; Zuidema et al. 2001; Peters 2003) employs a modification of the shear-induced crystallization model proposed by Eder and Janeschitz-Kriegl (1997) which provides a good correlation between the predicted flow-induced structures and experimental data and a recoverable strain model with a Leonov's driving force (Leonov 1976, 1987) for flow-induced crystallization that correlates most strongly with the viscoelastic mode corresponding to the largest relaxation time. Zuidema's model only includes the second invariant of the deviatoric part of the recoverable strain which is a measure of the molecular orientation, although no model for the molecular orientation was included in his flow-induced crystallization formulation.

The model of Kannan and Rajagopal (Kannan and Rajagopal 2005) treats the amorphous phase as a viscoelastic fluid, while the crystalline phase is assumed to behave as a transversally elastic material, uses a thermodynamic formulation, and requires a judicious choice of the free energy and other thermodynamic functions for predicting accurately the initiation of crystallization. If such a judicious choice is made, the model predicts necking phenomena at high drawing speeds.

The model proposed by Forest and Ueda (1999) uses Avrami's crystallization kinetics, a crystallization rate that depends on the difference between the ultimate and the current degrees of crystallization and the molecular orientation order parameter as suggested by Ziabicki (1976). For isothermal flows, the melt's dynamic viscosity is assume to depend in an exponential manner on the degree of crystallization, and the evolution equation for the uniaxial orientation along the fiber is nonlinearly coupled to both the flow-induced orientation and the flow-independent terms which take into account the intermolecular potential, and is consistent with Doi's nematodynamic theory (Doi and Edwards 1986). This model has been analyzed and extended by Forest et al. (1997a, b) and applied to the melt spinning of thermotropic liquid crystalline polymers by Zhou et al. (2000).

Some sample results obtained with a one-dimensional, one-phase model which is an extension of that of Zhou et al. (2000), are illustrated in Fig. 14.1 for different Biot numbers. The results presented in this figure have been nondimensionalized with respect to the temperature and axial velocity of the melt at the die's exit, the fiber's radius at the die's exit and the spinline length, and correspond to a nondimensional drawing speed equal to $\sqrt{100}$.

For the two smaller Biot numbers considered in Fig. 14.1, the results indicate that the fiber's axial velocity B increases in an exponential manner from the die's exit to the take-up drum, the temperature decreases in an almost linear manner, the degree of crystallization exhibits a sigmoid shape and reaches its ultimate value, i.e., 0.8, before the take-up drum location, and full molecular orientation is not achieved along the spinline. The exponential behavior of the axial velocity observed in Fig. 14.1 is analogous to that of isothermal, compound, liquid semi-crystalline fibers (Ramos 1999, 2002).

For the largest Biot number considered in Fig. 14.1, both the axial velocity and the degree of crystallization exhibit a sigmoid shape, the heat transfer losses are larger, the temperature decreases faster, and the degree of crystallization increases

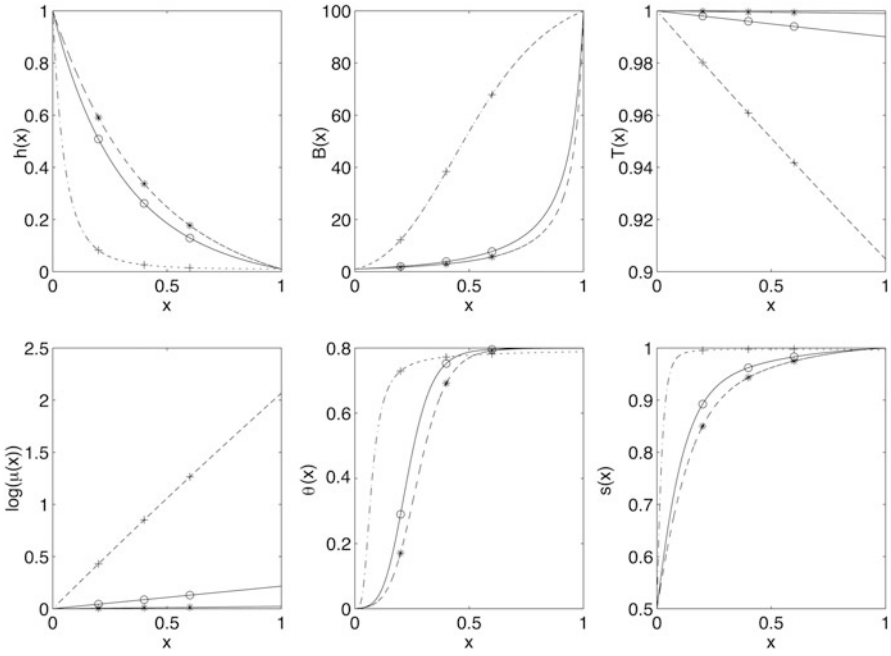

Fig. 14.1 Nondimensional fiber's radius (*top left*), axial velocity (*top middle*), temperature (*top right*), decimal logarithm of the dynamic viscosity (*bottom left*), degree of crystallization (*bottom middle*) and molecular orientation order parameter (*bottom right*) obtained with a one-dimensional, one-phase, fiber spinning model, for three different Biot numbers (The smallest and largest Biot numbers correspond to * and +, respectively)

faster than for the smaller Biot numbers. Figure 14.1 also indicates that, for the largest Biot number, complete molecular orientation and the ultimate degree of crystallization are achieved at locations equal to 0.50 and 0.25 times the spinline length, respectively, and that the logarithm of the dynamic viscosity increases in an almost linear manner.

Figure 14.1 also shows that, for the conditions considered, the increase in temperature associated with the latent heat of crystallization is small and cannot be observed; for larger values of the latent heat, the temperature first decreases from the die's exit up to an axial location where it increases, then reaches a relative maximum and then decreases. The location of this temperature peak is associated with the amorphous-to-crystalline phase transition. Both the location and peak of the temperature profile depend on the processing conditions, the pre-exponential factor and activation energy of the Arrhenius expression used to account for the dependence on the dynamic viscosity on temperature, and on the same factors for the relaxation time employed in the Maier-Saupe parameter. It also depends on the constants employed to account for the dependence of the dynamic viscosity law on the molecular orientation through Ziabicki's model of crystallization (Ziabicki 1974, 1976).

The effects of gravity, i.e., Froude number, and surface tension, i.e., the capillary number have been found to be small for drawing speeds typical of fiber spinning processes, although these effects may be important at low drawing ratios (George 2004).

The results presented in Fig. 14.1 as well as many others not shown here indicate that the accurate prediction of fiber spinning processes of liquid semi-crystalline polymers with one-dimensional models depends on many parameters even when using simple crystallization models, e.g., generalizations of the Avrami-Kolmogorov kinetics, and molecular orientation models characterized by an order parameter, even if a simple Newtonian rheology for the melt is used.

Figure 14.1 also shows that heat transfer losses have a great impact on the flow field and the degree of crystallization and molecular orientation. The fiber's contraction increases as the heat transfer losses are increased, and this contraction results in an increase of the strain rate which affects directly the molecular orientation; the latter in turn affects the degree of crystallization on two accounts. First, the thermal contribution to the crystallization increases as the temperature decreases, while the strain rate increase results in an increase of the flow-induced crystallization.

Since the approach employed in obtaining the results presented in Fig. 14.1 is based on a generalization of the Avrami-Kolmogorov kinetics described in Sect. 14.2, assumes a constant growth rate for both the thermal and flow-induced crystallizations, and the nucleation rate is assumed to be the sum of the thermal and flow-induced nucleation rates, where the former depends on the temperature and the latter on the strain rate, it is difficult to separate these two contributions as indicated in (14.8). For the conditions employed in Fig. 14.1, it was found that the contribution of the flow-induced crystallization was largest near the die's exit where the flow undergoes a large contraction but was comparable to the thermal one. The flow-induced crystallization was found to increase as the draw ratio was increased but was always found largest close to the die's exit.

14.5.1.2 Two-Phase Models

The two-phase isothermal model developed by Kulkarni and Beris (1998) includes Flory's approach (1947) for modelling the onset of crystallization. After the onset of crystallization, the amorphous phase is treated as a viscoelastic fluid represented by the White-Metzner rheological model, while the semi-crystalline phase is treated as an anelastic solid. The model predicts the necking phenomenon along the fiber at high drawing speeds which is attributed to structural changes induced by crystallization and the ability of the semi-crystalline phase to rapidly take up high stresses. However, several mechanics for necking at high spinning velocities have been proposed, e.g., viscous, viscoelastic and inertial mechanisms, and the radial distribution of the dynamic viscosity. Zahorski (1993) has shown that any radial viscosity distribution across the fiber intensifies the inertial mechanism and that, for sufficiently large radial viscosity variations across the fiber, a location reduction

in the axial velocity is not necessary for the onset of necking. The relevance of viscosity or viscoelasticity is not so clear, for one may not be able to determine the mechanism responsible for the local viscosity reduction associated with necking.

The two-phase model of Doufas et al. (2000a, b) and Doufas and McHugh (2001a) treats the amorphous phase as a Giesekus fluid and employs a rigid-rod model for the semicrystalline phase; the rigid rods are oriented by the flow, and both the amorphous and crystalline phases are coupled through the stress and momentum balance and feedback of the crystallinity to the melt's relaxation times. Their model also includes a Peterlin approximation in the evolution equation for the conformation tensor, and the relaxation times are assumed to be functions of both the temperature and the degree of crystallization which was modelled using Nakamura's kinetics, where the rate of crystallization depends on the temperature and the trace of the total stress tensor; the latter was assumed to be equal to the sum of those of the amorphous and crystalline phases, i.e., no volumetric effects were considered in determining the total stress tensor. A similar approach was followed by McHugh and Doufas (2001a) in their studies of fiber spinning of nylon and poly (ethylene terephtalate) (PET).

Doufas and McHugh model (2000a, b) and McHugh and Doufas (2001a) has been extended to include an extended pom-pom rheology (Kohler et al. 2005; Kohler and McHugh 2008) and to analyze the melt spinning of poly(lactic acid) which has more structure than PET and Nylon 6.6, and to include the whole spinline, so that the modified model avoids discontinuities generated by the imposition of continuation conditions at the crystallization temperature onset and excessive strength of the flow-induced crystallization compared with the quiescent one; the model also employs Avrami's kinetics (Shrikhande et al. 2006) for crystallization and has also been used to study the melt spinning of PP (Kohler and McHugh 2007) and multifilament melt spinning by accounting for the nonuniform quenching of the fibers (Jeon and Cox 2008; Dutta 2004).

14.5.2 Two-Dimensional Models of Fiber Spinning of Liquid Semi-Crystalline Polymers

The two-dimensional models described in this section are computationally demanding because they determine the flow, thermal, molecular orientation, crystallization and stress fields; they also determine the fiber's radius. At the fiber's free surface and, in the absence of evaporation, kinematic, dynamic and thermal boundary conditions must be satisfied. The kinematic condition is associated with the fact that the fiber's free surface is a material one, whereas the dynamic conditions establish that there is continuity of tangential stresses and the difference between the normal stresses on both sides of that surface must be balanced by surface tension which may depend on the temperature.

The surface tension contribution is proportional to the two radii of curvature of the free surface; one of them is the fiber's local radius while the other one depends on the second-order derivative of the fiber's radius with respect to the axial distance along the fiber. The accurate and stable discretization of the latter is not a trivial task, especially at high-drawing speeds when necking may appear in the fiber, as discussed above.

The thermal boundary conditions at the fiber's outer radius require continuity of the heat flux normal to that interface and is usually imposed by considering a film heat transfer coefficient and the difference between the temperature at that interface and that of the surroundings; the film transfer coefficient may also include radiation effects and depends on the fiber's velocity and the properties of the gases surrounding the fiber.

A more accurate model of the cooling of fibers should account for the boundary layer on the fiber so that the dynamics of the fiber are nonlinearly coupled to those of the surroundings. In such a model, in addition to the continuity of heat fluxes normal to the interface, the temperature must be continuous (Ramos 2005b, 2014). In these coupled two-dimensional models, no film heat transfer correlation is needed, although it may be determined from the results obtained by performing numerical experiments whereby the flow and thermal conditions for both the fiber and the gases that surround it are changed.

A fully two-dimensional numerical simulation of axisymmetric, isothermal, spinning flows of LCP based on the use of Doi's equations (Doi 1980, 1981; Doi and Edwards 1986) with a quadratic closure approximation was reported by Mori et al. (1997).

Numerical studies of the two-dimensional non-isothermal melt spinning of viscoelastic melts have been carried out by Joo et al. (2002) who employed a one-phase formulation where the crystallization kinetics is described by Nakamura's model, whereas the crystallization rate was modelled as per Ziabicki's formulation (Ziabicki 1974, 1976) and depends on both the temperature and the molecular orientation. The melt rheology was based on a Giesekus constitutive equation.

Joo et al.'s (2002) two-dimensional simulations indicate that, although the kinematics of fiber is approximately one-dimensional, the radial variations of temperature result in radial variations of the viscoelastic stresses across the fiber. This radial dependence, in turn, results in nonuniform molecular orientation and crystallization across the fiber. Their numerical experiments also indicate that the thermally-induced crystallization depends strongly on Avrami's exponent and that a sharp increase in crystallinity due to flow-induced crystallization is predicted to occur only when the polymer chains are highly aligned in the fiber's drawing direction at high spinning rates.

A similar model was developed by Sun et al. (2000) who used the Phan-Thien-Tanner rheological model.

14.5.3 Hybrid Models of Fiber Spinning of Liquid Semi-crystalline Polymers

Hybrid models of fiber spinning processes are also referred to as 1.5 dimensional models, use a one-dimensional equation for the axial velocity along the fiber and two-dimensional equations for the energy and stresses (Henson et al. 1998) and/or the conformation and the molecular orientation (Doufas and McHugh 2001b; McHugh and Doufas 2001b).

Henson et al. (1998) accounted for the radial temperature distribution across the fiber by means of a von Karman-Pohlhausen method with a parabolic temperature distribution and employed the average temperature across the fiber to evaluate the one-dimensional linear momentum equation, whereas Doufas and McHugh (2001b) and McHugh and Doufas (2001b) employed a two-dimensional formulation for the temperature and a one-dimensional formulation for the conformation and orientation tensors; only the diagonal components of the conformation and the orientation tensors along the fiber were considered in their formulation for elongational flows. The equations for these three variables are first-order partial differential equations and only require the specification of these three variables at an axial location along the fiber.

Ramos (2005b), Blanco-Rodríguez (2011) and Blanco-Rodríguez and Ramos (2011, 2012) developed a hybrid model for the fiber spinning of compound and hollow-compound liquid semi-crystalline fibers that consist of one-dimensional equations for the fiber's geometry and leading-order axial velocity component, and two-dimensional equations for the temperature, molecular orientation and crystallization; in such a formulation, the radial velocity depends linearly on the radial coordinate in accord with an asymptotic analysis of the continuity equation for slender incompressible fibers. The molecular orientation model was based on that of Doi and Edwards (1986), whereas the crystallization one employed Ziabicki's approximation (1976). These authors employ two formulations for the molecular orientation tensor; the first one determines the components of this tensor using a slender fiber approximation, whereas the second one uses an order parameter.

The results of the hybrid model proposed by Blanco-Rodríguez and Ramos (2012) were found to be in qualitative accord with those of a one-dimensional model that employs an order parameter for the molecular orientation, neglects axial heat conduction along the fiber and is only valid for slender fibers at low Reynolds and Biot numbers, but differences between the one- and two-dimensional models were observed near the die's exit where the fiber undergoes a large contraction and the strain rate is largest, and near the fiber's outer radius where cooling is important. In fact, these authors found that, even at moderately low Biot numbers, the temperature across the compound fiber is not uniform owing to heat losses as shown in Fig. 14.2 and that the temperature non-uniformities are mainly a function of the Biot number, the thermal conductivity and the pre-exponential factor and activation energy of the dynamic viscosity law for the cladding. The authors also

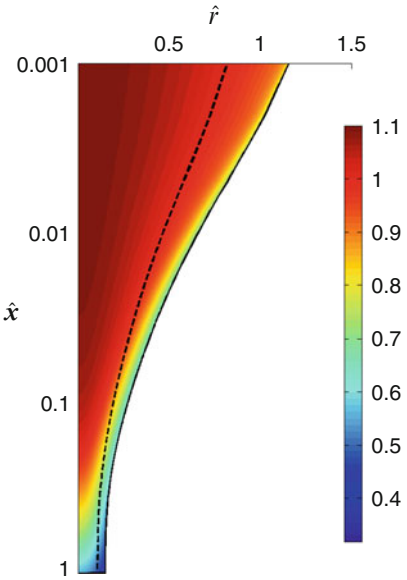

Fig. 14.2 Nondimensional temperature distribution in a semi-crystalline compound polymer fiber obtained with a hybrid model (The *dotted line* denotes the interface between the core and the cladding)

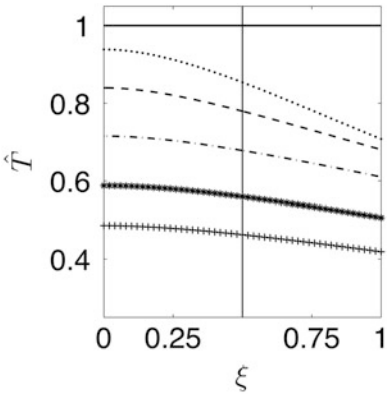

Fig. 14.3 Nondimensional temperature profile in a semi-crystalline compound polymer fiber obtained with a hybrid model (The *solid vertical line* denotes the interface between the core and the cladding)

found that the cross-sectional averaged temperature predicted by their two-dimensional model exhibits the same qualitative trends as those of an asymptotic one-dimensional model.

Figure 14.2 illustrates the nondimensional temperature distribution in a compound liquid semi-crystalline fiber and the cooling at the outer surface of the cladding. Along this surface, a thermal boundary layer is formed; the thickness of the layer increases with the distance along the fiber and the temperature across the fiber becomes nearly uniform when the fiber solidifies. This is also clearly observed in Figs. 14.3 and 14.4 which show the nondimensional temperature profiles at several locations along a compound and a hollow compound fiber, respectively.

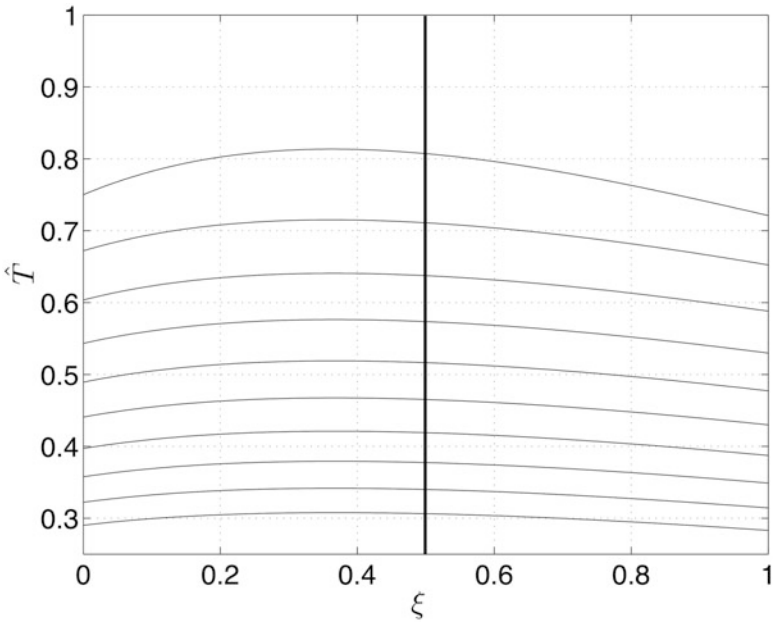

Fig. 14.4 Nondimensional temperature profile in a semi-crystalline hollow compound polymer fiber obtained with a hybrid model (The *solid vertical line* denotes the interface between the inner and outer annular fibers)

The temperature at the die's exit was assumed to be uniform in Figs. 14.2, 14.3, and 14.4, and this temperature was used to nondimensionalize the temperature distributions observed in these figures. Furthermore, in Figs. 14.3 and 14.4, the radial coordinate was nondimensionalized by the fiber's local radius in order to clearly observe the thermal boundary layers at the free surfaces of the fiber, and the temperature gradients at the interface between the core and the cladding and between the two annular fibers in compound and hollow compound fibers, respectively.

The results presented in Fig. 14.5 indicate that, for the conditions considered here, both the core and the cladding of liquid semi-crystalline compound polymer fibers reach almost complete molecular orientation close to the die's exit, and that the core reaches complete orientation earlier than the cladding because of the heat transfer losses at the cladding's outer surface which increase the thermal and flow-induced crystallization rates.

In both one- and two-dimensional and hybrid models of compound and hollow-compound liquid semi-crystalline fibers, almost full molecular orientation was observed close to the die's exit due to the large strain rate there and the fact that the Doi-Edwards molecular model and the Maier-Saupe potential predict an increase of the molecular orientation as the strain rate and velocity gradient increase.

At low Biot numbers, Blanco-Rodríguez and Ramos (2012) observed that, depending on the activation energies employed for the relaxation time and the

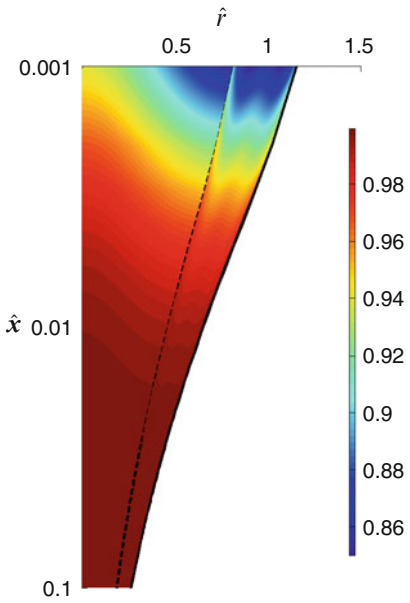

Fig. 14.5 Molecular orientation order parameter in a semi-crystalline compound polymer fiber obtained with a hybrid model (The *dotted line* denotes the interface between the core and the cladding)

activation energy of the Arrhenius expression for the dynamic viscosity law, the order parameter for the molecular orientation first increases until it reaches a constant value and then decreases even when the fiber solidifies. As stated above, this behavior is unphysical and was corrected by modifying the Maier-Saupe potential in the transport equation for either the molecular orientation tensor or the molecular orientation order parameter.

Figure 14.6 illustrates the degree of crystallization in both the core and the cladding of a semi-crystalline compound fiber and indicates that, for the conditions considered here, very little crystallization occurs in the cladding and that the core reaches almost full orientation before the fiber is taken up at the collecting drum. For the conditions considered in Figs. 14.2 and 14.6, the flow-induced crystallization was found to be smaller than the thermal one.

As stated previously, a one-dimensional approximation to the continuity and linear momentum equations is only strictly valid for slender fibers at low Reynolds numbers. Moreover, the leading-order temperature in an asymptotic expansion of the flow and thermal fields in terms of the slenderness ratio is uniform across the fiber and this demands that the Biot number at the fiber's outer surface be sufficiently small, so that the leading-order boundary condition corresponds to an adiabatic surface. If one were to obtain the radial dependence of the temperature for slender fibers, one should proceed to higher order in the asymptotic expansion or employ a two-dimensional model.

Some researchers, e.g., Zahorski (1990) have shown that, independently of the magnitude of the radial and axial viscosity gradients, the velocity profiles across a fiber are always convex, i.e., the velocity gradient is always negative at the fiber's outer surface at least in regions where the polymer is in the liquid state.

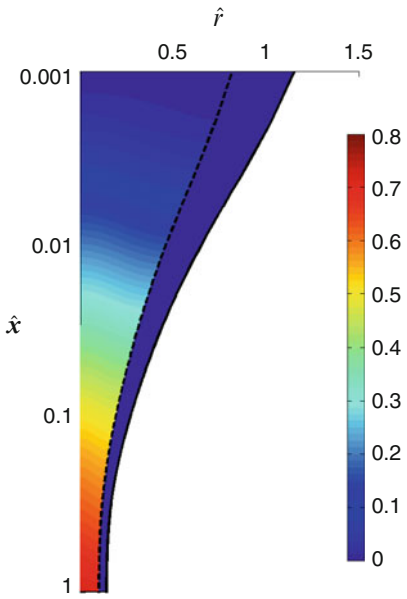

Fig. 14.6 Degree of crystallization in a semi-crystalline compound polymer fiber obtained with a hybrid model (The *dotted line* denotes the interface between the core and the cladding)

The hybrid models developed to-date make use of the one-dimensional equations obtained from either asymptotic methods in terms of the slenderness ratio or Taylor's series expansions in the radial coordinate and employ effective properties that take into account the radial variations of the temperature, stresses, molecular orientation and crystallization by performing cross-sectional averages for these variables.

The great advantage of hybrid methods compared with two-dimensional ones is that they employ one-dimensional equations for the fiber's radius and average axial velocity component along the fiber, and, therefore, they avoid the cost of and the difficulties encountered in two-dimensional models when applying kinematic and dynamic boundary conditions at the fiber's free surface; in addition, they may provide approximate two-dimensional distributions of the molecular orientation, crystallization, temperature and stresses. However, they are not strictly consistent with an asymptotic analysis of slender fibers at low Reynolds numbers and employ a radial velocity component that, at leading-order, is a linear function of the radial coordinate; moreover, the leading-order pressure is independent of the radial coordinate.

14.6 Conclusions and Future Work

A review of one- and two-dimensional and hybrid models of the melt spinning of LCP and liquid semi-crystalline polymer fibers has been presented. Most of the models developed to-date are one-dimensional; two-dimensional models are computationally costly and require to determine the fiber's surface where kinematic,

dynamic and thermal boundary conditions must be satisfied, as part of the solution. Hybrid models avoid the imposition of dynamic boundary conditions at the fiber's free-surface by employing a one-dimensional formulation for the fiber's geometry and axial velocity component, and a two-dimensional formulation for the molecular, thermal and crystallization fields. Albeit hybrid models reduce to one-dimensional ones when the properties are uniform across each section of the fiber, they are based on one-dimensional formulations that are strictly applicable to slender fibers at low Reynolds and Biot numbers. These conditions imply that the heat transfer losses at the fiber's outer surface should be small. This may be the case in some fiber spinning processes, but it may not be so at high cooling rates. This means that, although hybrid models may be more accurate than one-dimensional ones, the use of averaged effective properties, e.g., viscosity, temperature, molecular orientation, crystallization, etc., in the one-dimensional linear momentum equation may be a coarse approximation that accounts in an integrated manner for the radial dependence of the axial velocity field. Furthermore, the slenderness approximation implies that, at leading-order, the radial velocity component is a linear function of the radial coordinate and, therefore, the flow is mainly uniaxial.

The crystallization models that have been employed in the study of fiber spinning of liquid semi-crystalline fibers are mainly based on the Avrami-Kolmogorov-Johnson-Mehl-Evans kinetics which was developed for quiescent isothermal crystallization. This model has been generalized to include flow-induced crystallization which may depend on the stresses, strain rate, normal stress difference, pressure, etc. However, it is as yet unknown which of these has the strongest influence and under what conditions on crystallization.

Perhaps the most detailed model of crystallization employed in fiber spinning processes is the one developed by Schneider et al. (1988) with the flow-induced crystallization model of Eder and Janeschitz-Kriegl (1997). However, it has been shown in this chapter that Schneider's model is based on the Avrami-Kolmogorov kinetics and derivatives thereof. This means that the model is subjected to the same criticisms as the original Avrami-Kolmogorov formulation. Furthermore, Schneider's model assumes that the dimensionality constant for crystal growth that appears in the original Avrami-Kolmogorov' formulation is an integer; however, quiescent crystallization experiments indicate that this may not be the case and that such a constant may not be an integer.

Most of the molecular orientation models for fiber spinning of liquid semi-crystalline polymers developed to-date have been based on the reptation model and the probability distribution formulation developed by Doi and Edwards (1986) and the intermolecular potential of Maier and Saupe (1958) that provide a transport equation for the order/structure/orientation tensor upon approximating the fourth-order moments in terms of the second-order ones.

One-dimensional models that use a uniaxial flow approximation have shown that the molecular orientation order parameter may first increase, reach a relative maximum, and then decrease. Such a behavior has been attributed to the Maier-Saupe potential when only one relaxation time is considered, as one can easily deduce by studying the fixed points of the transport equation for the molecular order

parameter. Although such a shortcoming may be eliminated by appropriately modifying the Maier-Saupe potential, there is a clear need for including not only the longest relaxation times that characterizes the tail of the distribution function, but many others as well.

The weakest points of the one- and two-dimensional and hybrid models for fiber spinning developed to-date are those associated with the effects of the molecular orientation on the crystallization and the effects of the latter on the former, as well as those of the crystallization and orientation on the melt's rheology and, therefore, on the flow field which in turn affect the molecular orientation and crystallization rates. Many of the models that couple the molecular orientation and crystallization assume that the crystallization rate depends on the temperature and molecular orientation, whereas the latter depends on the strain rate, temperature and relaxation time. Clearly, the molecular orientation should also depend on the crystallization.

The transport equations for the molecular orientation tensor or order parameter and the degree of crystallization developed to-date are first-order differential equations of the hyperbolic type and, therefore, only require one boundary condition in the radial and axial directions. This means that, when these equations are used in a one-dimensional model for fiber spinning of liquid semi-crystalline fibers, the molecular orientation and crystallization depend on the values of these variables at the die's exit, as well as on the flow and temperature fields: however, when used in two-dimensional or hybrid models, one should account for the direction of the characteristic lines of these equations, and this implies that one should account for both the axial and radial velocity components when imposing boundary conditions. The hyperbolic character of the transport equations for the molecular may make them not to be applicable to compound or hollow-compound fibers due to the interfaces between the core and the cladding in the former and the interface between the two annular fibers in the latter. At such interfaces, one should expect an interaction between the polymers of, for example, the core and cladding.

The molecular orientation and crystallization models may not even be valid for the fiber spinning of round fibers consisting of only one material because at the fiber's free surface where cooling is important, one should expect that the crystallization and molecular orientation are affected by the heat transfer losses, while, at the fiber's axis, these variables satisfy symmetry conditions. This means that a more physically realistic model for the fiber spinning of liquid crystalline polymers should include diffusion-like terms in the transport equations for the structure tensor and the crystallization. A model that accounts for the interactions between two similar or dissimilar materials at the interfaces of compound and hollow-compound fibers is also needed. Such a model must take into account the orientation and organization of macromolecules at interfaces that may lead to the formation of interphases. The creation of such interphases involves physical, chemical and physicochemical mechanisms.

A full model of fiber spinning processes should also account for the dynamics and thermal field of the gases that surround the fiber, so that there is no need for film heat transfer correlations that are employed in the models developed to-date. Most of these heat transfer correlations have been obtained in very specific experimental

setups and for very specific materials and operating conditions, and may not be strictly applicable in another scenarios or when the processing of other materials is considered.

Since the flow, molecular orientation, crystallization and thermal fields in fiber spinning of LCP are history-dependent, a more accurate model should include the melt's dynamics in the die and the flow relaxation from its confinement in the die to the free-surface conditions of the fiber. This would allow to account for possible swell effects near the die's exit. In addition, the predictions of any fiber spinning model should be tested with experimental data under different operating conditions and for a variety of polymers in order to accurately determine the parameters and constants that appear in such a model as well as their dependence on the material being processed and the operating conditions.

Acknowledgements The writing of this chapter was supported by Project FIS2012-38430 from the Ministerio de Economía y Competitividad of Spain. The author is grateful to many colleagues who provided many suggestions on the different versions of this manuscript.

References

Avrami A (1939) Kinetics of phase change. I. General theory. J Chem Phys 7:1103–1112
Avrami A (1940) Kinetics of phase change. II. Transformation-time relations for random distribution of nuclei. J Chem Phys 8:212–224
Avrami A (1941) Kinetics of phase change. III. Granulation, phase change, and microstructure. J Chem Phys 9:177–184
Ball JM, Majumdar A (2010) Nematic liquid crystals: from Maier-Saupe to a continuum theory. Mol Cryst Liq Cryst 525:1–11
Betchel SE, Forest MG, Holm DD, Lin KJ (1988) 1-D closure models for 3-D incompressible viscoelastic free jets: von Karman flow geometry and elliptical cross-section. J Fluid Mech 196:241–262
Betchel SE, Bolinger KD, Cao JZ, Forest MG (1995) Torsional effects in higher order viscoelastic thin-filament models. SIAM J Appl Math 55:58–99
Bhave AV, Menon RK, Armstrong RC, Brown RA (1993) A constitutive equation for liquid crystalline polymer solutions. J Rheol 37:413–441
Blanco-Rodríguez FJ (2011) Numerical simulation of the molecular orientation and degree of crystallization of semi-crystalline fibres. Ph.D. thesis, Universidad de Málaga, Málaga, Spain
Blanco-Rodríguez FJ, Ramos JI (2011) Melt spinning of semi-crystalline compound fibers. Polymer 52:5573–5586
Blanco-Rodríguez FJ, Ramos JI (2012) A simplified two-dimensional model of the melt spinning of semi-crystalline hollow compound fibers. Int J Thermal Sci 58:102–112
Burger M, Capasso V, Eder G (2002) Modelling of polymer crystallization in temperature fields. Z Angew Math Mech (ZAMM) 82:51–63
Capasso V (2003) Mathematical modelling for polymer processing. Springer, New York
Chawla KK (1998) Fibrous materials. Cambridge University Press, New York
Cocchini F, Aratari C, Marrucci G (1990) Tumbling of rodlike polymers in the liquid-crystalline phase under shear flow. Macromolecules 23:4446–4451
Coppola S, Grizzuti N, Maffettone PL (2001) Microrheological modeling of flow-induced crystallization. Macromolecules 34:5030–5036

Coppola S, Balzano L, Gioffredi E, Maffettone PL, Grizzuti N (2004) Effects of the degree of undercooling on flow induced crystallization in polymer melts. Polymer 45:3249–3256
de Gennes PG (1974) The physics of liquid crystals. Oxford University Press, Oxford
Denn MM, Petrie CJS, Avenas P (1975) Mechanics of steady spinning of a viscoelastic liquid. AIChE J 21:791–795
Di Lorenzo ML, Silvestre C (1999) Non-isothermal crystallization of polymers. Prog Polym Sci 24:917–950
Doi M (1980) Rheological properties of rodlike polymers in isotropic and liquid crystalline phases. Ferroelectrics 30:247–254
Doi M (1981) Molecular dynamics and rheological properties of concentrated solutions of rodlike polymers in isotropic and liquid crystalline phases. J Polym Sci Polym Phys 19:229–243
Doi M, Edwards SF (1986) The theory of polymer dynamics. Oxford University Press, New York
Doufas AK, McHugh AJ (2001a) Simulation of melt spinning including flow-induced crystallization. Part III. Quantitative comparisons with PET spinline data. J Rheol 92:403–420
Doufas AK, McHugh AJ (2001b) Two-dimensional simulation of melt spinning with a microstructural model for flow-induced crystallization. J Rheol 45:855–879
Doufas AK, Dairanieh IS, McHugh AJ (1999) A continuum model for flow-induced crystallization of polymer melts. J Rheol 43:85–109
Doufas AK, McHugh AJ, Miller C (2000a) Simulation of melt spinning including flow-induced crystallization. Part I. Model developments and predictions. J Non-Newtonian Fluid Mech 92:27–66
Doufas AK, McHugh AJ, Miller C, Immaneni A (2000b) Simulation of melt spinning including flow-induced crystallization. Part II. Quantitative comparisons with industrial spinline data. J Non-Newtonian Fluid Mech 92:81–103
Dutta A (2004) Melt spinning of (multifilament) poly(ethylene terephthalate) fibers: a simulation approach. Polym Eng Sci 27:1050–1058
Eder G (1997) Macromolecular design of polymeric materials. Marcel Dekker, New York
Eder G, Janeschitz-Kriegl H (1997) Crystallization. In: Meijer HEH (ed) Materials science and technology: a comprehensive treatment, processing of polymers, vol 18. VCH, Weinheim, pp 269–342
Eder G, Janeschitz-Kriegl H, Liedauer S (1990) Crystallization processes in quiescent and moving polymer melts under heat transfer conditions. Prog Polymer Sci 15:629–714
Ericksen JL (1960) Anisotropic fluids. Arch Rat Mech Anal 4:231–237
Ericksen JL (1991) Liquid crystals with a variable degree of orientation. Arch Rat Mech Anal 113:97–120
Evans RU (1945) The law of expanding circles and spheres in relation to the lateral growth of surface films and the grain-size of metals. Trans Faraday Soc 41:365–374
Flory PJ (1947) Thermodynamics of crystallization in high polymers I. Crystallization induced by stretching. J Chem Phys 15:397–408
Forest MG, Ueda T (1999) An isothermal model for high-speed spinning of liquid crystalline polymer fibers: coupling of flow, orientation, and crystallization. J Non-Newtonian Fluid Mech 84:109–121
Forest MG, Wang Q (2003) Monodomain response of finite-aspect-ratio macromolecules in shear and related linear flows. Rheol Acta 42:20–46
Forest MG, Wang Q, Bechtel SE (1997a) One dimensional isothermal spinning models for liquid crystalline polymer fibers. J Rheol 41:821–850
Forest MG, Wang Q, Bechtel SE (1997b) 1-D models for thin filaments of liquid-crystalline polymers: coupling of orientation and flow in the stability of simple solutions. Phys Nonlinear Phenom 99:527–544
Forest MG, Zhou R, Wang Q (2002) Symmetries of the Doi kinetic theory for nematic polymers of arbitrary aspect ratio: at rest and linear flows. Phys Rev E 66:031712
Forest MG, Zhou R, Wang Q (2003) Full-tensor alignment criteria for sheared nematic polymers. J Rheol 47:105–127

Forest MG, Zhou R, Wang Q (2004) Scaling behavior of kinetic orientational distributions for dilute nematic polymers in weak shear. J Non-Newtonian Fluid Mech 116:183–204
Fukuda T, Rudolp P, Uda S (eds) (2004) Fiber crystal growth from the melt. Springer, New York
Gagon DK, Denn MD (2004) Computer simulation of steady polymer melt spinning. Polym Eng Sci 21:844–853
George HH (2004) Model of steady-state melt spinning at intermediate take-up speeds. Polym Eng Sci 22:292–299
Giesekus H (1982) A simple constitutive equation for polymer fluids based on the concept of deformation-dependent tensorial mobility. J Non-Newtonian Fluid Mech 11:69–109
Glicksman LR (1968) The dynamics of a heated free jet of variable viscosity liquid at low Reynolds number. ASME J Fluids Eng 90:343–354
Greco F, Marrucci G (1993) Flow behavior of liquid crystalline polymers. Adv Chem Phys 86:331–401
Henson GM, Cao D, Bechtel SE, Forest MG (1998) A thin-filament melt spinning model with radial resolution of temperature and stress. J Rheol 42:329–360
Hoffman JD, Miller RL (1997) Kinetics of crystallization from the melt and chain folding in polyethylene fractions revisited: theory and experiment. Polymer 38:3151–3212
Hütter M (2004) Crystallization under external pressure. J Non-Newtonian Fluid Mech 120:55–68
Hütter M, Karlin IV, Öttinger HC (2003) Dynamic mean-field models from a nonequilibrium thermodynamic perspective. Phys Rev E 68:016115
Hyunh BP, Tanner RI (1983) Study of the non-isothermal glass fiber drawing process. Rheol Acta 22:482–499
Janeschitz-Kriegl H (2003) How to understand nucleation in crystallizing polymer melts under real processing conditions. Colloid Polym Sci 28:1157–1171
Jeon YP, Cox CL (2008) Modeling of multifilament PET fiber melt-spinning. J Appl Polym Sci 110:2153–2163
Johnson WA, Mehl RF (1939) Reaction kinetics in processes of nucleation and growth. Trans AIME 135:416–442
Joo YL, Sun J, Smith MD, Armstrong RC, Brown RA, Ross RA (2002) Two-dimensional numerical analysis of non-isothermal melt spinning with and without phase transition. J Non-Newtonian Fluid Mech 102:37–70
Kannan K, Rajagopal KR (2005) Simulation of fiber spinning including flow-induced crystallization. J Rheol 49:683–703
Kase S, Matsuo T (1965) Studies of melt spinning. I. On the stability of melt spinning. J Polym Sci A 3:2541–2554
Keller A, Kolnaar H (1998) Flow-induced orientation and structure formation, Chapter 4. In: Meiejer HEH (ed) Materials science and technology polymer processing. VCH Verlagsgesellschaft mbH/Wiley, Weinheim, pp 187–268
Kim KH, Aida R, Kang YA, Ikaga T, Ohkoski Y, Wataoka I, Urakawa H (2012) Effect of drawing stress on mesophase structure formation of poly(ethylene 2,6-naphthalane dicarboxylate) fiber just after the neck-drawing point. Polymer 53:4272–4279
Kohler WH, McHugh AJ (2007) Sensitivity analysis of low-speed melt spinning of isoctatic polypropylene. Chem Eng Sci 62:2690–2697
Kohler WH, McHugh AJ (2008) Prediction of the influence of flow-enhanced crystallization on the dynamics of fiber spinning. Polym Eng Sci 2008:88–96
Kohler WH, Shrikhande P, McHugh AJ (2005) Modeling melt spinning of PLA fibers. J Macromol Sci B 44:185–202
Kolmogorov AN (1937) On the statistical theory of the crystallization of metals. Bulletin of the Academy of Sciences of the USSR, Mathematical Series 1:355–359
Kulkarni JA, Beris AN (1998) A model for the necking phenomenon in high-speed fiber spinning based on flow-induced crystallization. J Rheol 42:971–994
Landau LD, Lifshitz EM (1980a) Statistical physics: part 1. Pergamon, New York
Landau LD, Lifshitz EM (1980b) Statistical physics: part 2. Pergamon, New York

Lauritzen JI, Hoffman JD (1960) Theory of formation of polymer crystals with folded chains in dilute solution. J Res Nat Bureau Stand 64A:73–102
Lauritzen JI, Hoffman JD (1973) Extension of theory of growth of chain folded polymer crystals to large undercoolings. J Appl Phys 44:4340–4352
Leonov AI (1976) Nonequilibrium thermodynamics and rheology of viscoelastic polymer media. Rheol Acta 15:85–98
Leonov AI (1987) On a class of constitutive equations for viscoelastic fluids. J Non-Newtonian Fluid Mech 25:1–59
Leslie FM (1968) Some constitutive equations for liquid crystals. Arch Rat Mech Anal 28:265–283
Leslie FM (1979) Theory of flow phenomena in liquid crystals. Adv Liq Cryst 4:1–81
Lin YH (2010) Polymer viscoelasticity. World Scientific, Singapore
Long D, Morse DC (2002) A Rouse-like model of liquid crystalline polymer melts: director dynamics and linear viscoelasticity. J Rheol 42:49–92
Long Y, Shanks RA, Stachurski ZH (1995) Kinetics of polymer crystallisation. Prog Polym Sci 20:651–701
Maffetone PL, Marrucci G, Mortier M, Moledaers P, Mewis J (1994) Dynamic characterization of liquid crystalline polymers under flow-aligning shear conditions. J Chem Phys 100:7736–7743
Maffetone PL, Sonnet AM, Virga EG (2000) Shear-induced biaxiality in nematic polymers. J Non-Newtonian Fluid Mech 90:283–297
Maier W, Saupe A (1958) Eine einfache molekulare theorie des nematischen kristallinflussigen zustandes. Z Naturforsch A 13:564
Maier W, Saupe A (1959) Eine einfache molekular-statistische theorie der nematischen kristallin-flussigen phase. 1. Z Naturforsch A 14:882–889
Maier W, Saupe A (1960) Eine einfache molekular-statistische theorie der nematischen kristallin-flussigen phase. 2. Z Naturforsch A 15:287–292
Marrucci G (1991) Rheology of rodlike polymers in the nematic phase with tumbling or shear orientation. Macromolecules 24:4176–4182
Marrucci G (1996) Dynamics of entanglements: a non-linear model consistent with the Cox-Merz rule. J Non-Newtonian Fluid Mech 62:679–689
Marrucci G, Maffetone PL (1989) Description of the liquid-crystalline phase of rodlike polymers at high shear rates. Macromolecules 22:4076–4082
Matovich MA, Pearson JRA (1969) Spinning a molten threadline: steady-state isothermal viscous flows. Ind Chem Eng Fund 8:512–520
McHugh AJ, Doufas AK (2001a) Modeling flow-induced crystallization in fiber spinning. Compos Appl Sci Manuf 32:1059–1066
McHugh AJ, Doufas AK (2001b) Simulations of fiber spinning and film blowing based on a molecular/continuum model for flow-induced crystallization. Korea-Australia Rheol J 13:1–12
Mori N, Hamaguchi Y, Nakamura K (1997) Numerical simulation of the spinning flow of liquid crystalline polymers. J Rheol 41:1095–1104
Nakamura K, Watanabe T, Katayama K, Amano T (1972) Some aspects of non-isothermal crystallization of polymers I. J Appl Polym Sci 16:1077–1091
Onsager L (1949) The effects of shape on the interaction of colloidal particles. Ann NY Acad Sci 51:627–659
Öttinger HC (1999) A thermodynamically admissible reptation model for fast flows of entangled polymers. J Rheol 43:1461–1493
Pantani R, Coccorullo I, Speranza V, Titomanlio G (2005) Modeling the morphology evolution in the injection molding of thermoplastic polymers. Prog Polym Sci 30:1185–1222
Pattamaprom C, Larson RG, van Dyke J (2000) Quantitative predictions of linear viscoelastic rheological properties of entangled polymers. Rheol Acta 39:517–531
Pattamaprom C, Larson RG, Sirivat A (2008) Determining polymer molecular weight distributions from rheological properties using the dual-constraint model. Rheol Acta 47:689–700
Pearson JRA (1985) Mechanics of polymer processing. Elsevier Applied Sciences, New York

Peters GWM (2003) A computational model for processing of semicrystalline polymers: the effects of flow-induced crystallization, Chapter 17. In: Sommer J-U, Reiter G (eds) Polymer crystallization. Lecture notes in physics, vol 606. Springer, Berlin, pp 312–324
Piorkowska E, Galeski A, Haudin JM (2006) Critical assessment of overall crystallization kinetics theories and predictions. Prog Polym Sci 31:549–575
Ramalingam S, Armstrong RC (1993) Analysis of isothermal spinning of liquid crystalline polymers. J Rheol 37:1141–1169
Ramos JI (1999) Asymptotic analysis of compound liquid jets at low Reynolds numbers. Appl Math Comput 100:223–240
Ramos JI (2001a) Nonlinear dynamics of hollow, compound jets at low Reynolds numbers. I J Eng Sci 39:1289–1314
Ramos JI (2001b) Drawing of annular liquid jets at low Reynolds numbers. Comput Theor Polymer Sci 11:429–443
Ramos JI (2002) Compound liquid jets at low Reynolds numbers. Polymer 43:2889–2896
Ramos JI (2005a) Modelling of liquid crystalline compound fibres. Polymer 46:12612–12625
Ramos JI (2005b) Convection and radiation effects in hollow, compound optical fibers, I. J Thermal Sci 44:832–850
Ramos JI (2006) Mathematical models of compound, polymer optical fibers, Chapter 7. In: Bregg RK (ed) Polymer research developments. Nova Science, New York, pp 127–185
Ramos JI (2007) Thermal analysis of bicomponent amorphous fibres. Appl Thermal Eng 27:586–598
Ramos JI (2014) Heat transfer processes in film casting of compressible polymers, Paper ICHTC15-9814. In: Proceedings of the 15th international heat transfer conference, ICHMT Digital Library. Begell House, New York
Rao IJ, Rajagopal RK (2002a) A thermodynamic framework for the study of crystallization in polymers. Z Angew Math Phys (ZAMP) 53:365–406
Rao IJ, Rajagopal RK (2002b) On the modeling of quiescent crystallization of polymer melts. Polymer Eng Sci 44:123–130
Rienacker G, Hess S (1999) Orientational dynamics of nematic liquid crystals under shear flow. Phys A 267:294–321
Rouse PE (1953) A theory of the linear viscoelastic properties of dilute solutions of coiling polymers. J Chem Phys 21:1271–1281
Schneider W, Köppl A, Berger J (1988) Non-isothermal crystallization. Int Polymer Process 2:151–154
Schultz JM (2001) Polymer crystallization. Oxford University Press, New York
Schultz WW, Davis SH (1982) One-dimensional liquid fibers. J Rheol 26:331–345
See H, Doi M, Larson RG (1990) The effect of steady flow fields on the isotropic-nematic phase transition of rigid rod-like polymers. J Chem Phys 92:792–800
Shanon JM, Schultz JM, Hsiao BS (2000) Structure development in the early stages of crystallization during melt spinning. Polymer 43:1873–1875
Shrikhande P, Kohler WH, McHugh AJ (2006) A modified model and algorithm for flow-enhanced crystallization—application to fiber spinning. J Appl Polym Sci 100:3240–3254
Strobl G (2006) Crystallization and melting of bulk polymers: new observations, conclusions and a thermodynamic scheme. Prog Polym Sci 31:398–442
Sun J, Subbiah S, Marchal JM (2000) Numerical analysis of nonisothermal viscoelastic melt spinning with ongoing crystallization. J Non-Newtonian Fluid Mech 93:133–151
Tanner RI (2002) A suspension model for low shear rate polymer solidification. J Non-Newtonian Fluid Mech 102:397–408
Tanner RI (2003) On the flow of crystallizing polymers. I. Linear regime. J Non-Newtonian Fluid Mech 112:251–268
Tanner RI, Qi F (2005) A comparison of some models for describing polymer crystallization at low deformation rates. J Non-Newtonian Fluid Mech 127:131–141

Vaish N, Cinader DK, Burghardt WR, Zhou W, Kornfield JA (2001) Molecular orientation in quenched channel flow of a flow aligning main chain thermotropic liquid crystalline polymer. Polymer 42:10147–10153

van Drongelen M, van Erp TB, Peters GWM (1988) Quantification of non-isothermal, multi-phase crystallization of isotactic polypropylene: the influence of the cooling rate and pressure. Int Polymer Process 2:151–154

van Meerveld J (2005) Model development and validation of rheological and flow induced crystallization: models for entangled polymer melts. Ph.D. Thesis, ETH Zürich, Switzerland

van Meerveld J, Hütter M, Peters GWM (2008) Continuum model for the simulation of fiber spinning, with quiescent and flow-induced crystallization. J Non-Newtonian Fluid Mech 150:177–195

Vassilatos G, Schmelzer ER, Denn MM (1992) Issues concerning the rate of heat transfer from a spinline. Int Polymer Process 7:144–150

Vrentas JS, Vrentas CM (2004) Theoretical aspects of fiber spinning. J Appl Poly Sci 93:986–993

Wang Q (1997) Biaxial steady states and their stability in shear flows of liquid crystal polymers. J Rheol 41:943–970

Zachmanoglou EC, Thoe DW (1986) Introduction to partial differential equations with applications. Dover, New York

Zahorski S (1990) An alternative approach to non-isothermal melt spinning with axial and radial viscosity distributions. J Non-Newtonian Fluid Mech 36:71–83

Zahorski S (1993) Necking in non-isothermal high-speed spinning with radial velocity variation. J Non-Newtonian Fluid Mech 50:65–77

Zheng R, Kennedy PK (2004) A model for post-flow induced crystallization: general equations and predictions. J Rheol 48:823–842

Zhou H, Forest MG, Wang Q (2000) Thermotropic liquid crystalline fibers. SIAM J Appl Math 60:1177–1204

Ziabicki A (1974) Theoretical analysis of oriented and non isothermal crystallization. Colloid Polym Sci 252:207–221

Ziabicki A (1976) Fundamentals of fibre formation. Wiley, New York

Ziabicki A, Jarecki L (2007) Crystallization-controlled limitations of melt spinning. J Appl Polym Sci 105:215–223

Ziabicki A, Jarecki L, Sorrentino A (2013) The role of flow-induced crystallization in melt spinning. e-Polymers 4:823–836

Zuidema H (2000) Flow-induced crystallization of polymers. Ph.D. Thesis, University of Technology Eindhoven, The Netherlands

Zuidema H, Peters GWM, Meijer HEH (2001) Development and validation of a recoverable strain-based model for flow-induced crystallization of polymers. Macromol Theory Simul 10:447–460